The Abdus Salam
International Centre for Theoretical Physics

United Nations
Educational, Scientific
and Cultural Organization

International Atomic
Energy Agency

World Year of PHYSICS 2005

SMR.1664 - 3

Conference on Single Molecule Magnets and Hybrid Magnetic Nanostructures

27 June - 1 July 2005

Application of High-Frequency Electron Paramagnetic Resonance to Studies of Single-Molecule Magnets

Stephen HILL
University of Florida
Department of Physics
P.O. Box 118440
392 3591
Gainesville, FL 32611-8440
U.S.A.

Application of high-frequency electron paramagnetic resonance to studies of single-molecule magnets

Stephen Hill

Department of Physics, University of Florida, Gainesville, FL32611

PART I - Introduction

- Single-molecule magnets
  - Emphasis on quantum magnetization dynamics

PART II - Experimental

- Overview of the high-frequency EPR technique
- The National High Magnetic Field Laboratory

PART III - Examples

- Symmetry of quantum tunneling in various Mn_{12} complexes
- Origin of fast quantum relaxation in Ni_4 complexes
- Quantum entanglement in $[Mn_4]_2$ dimers

Supported by: NSF, Research Corporation, NHMFL, & University of Florida

The first single molecule magnet: Mn_{12}-acetate

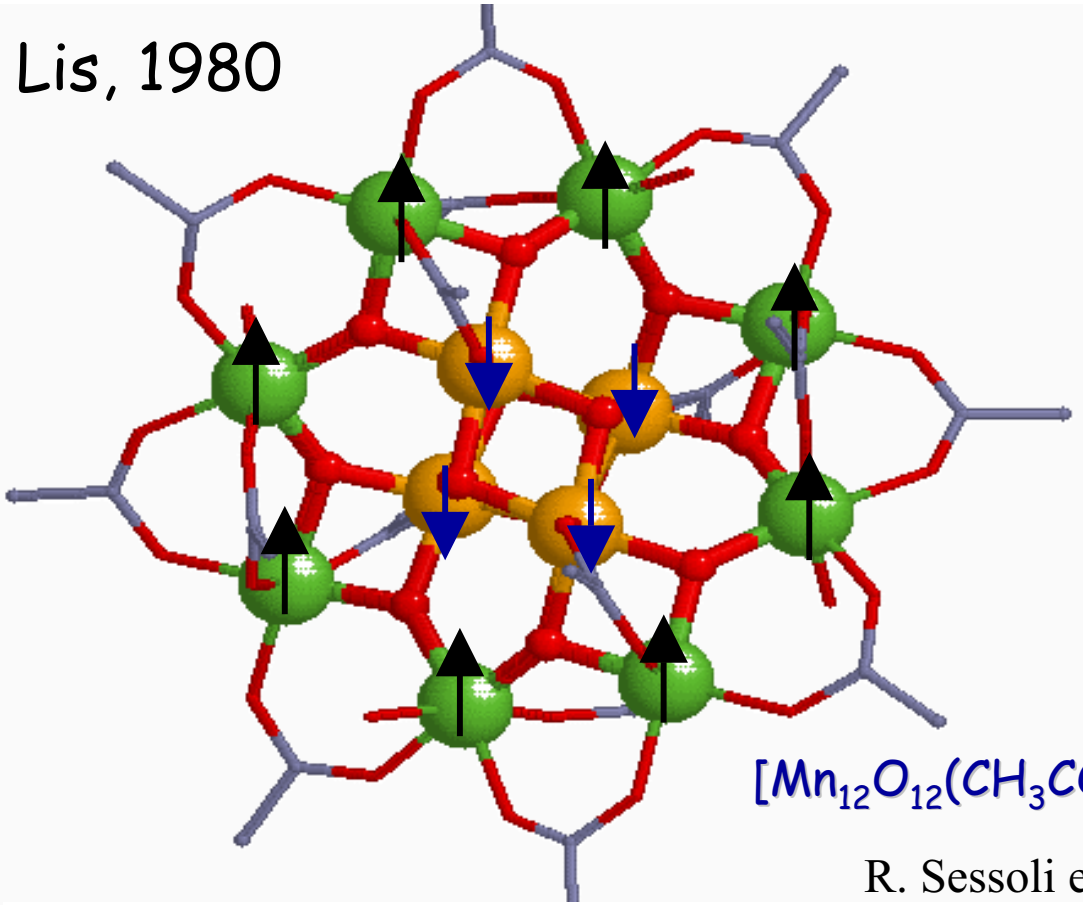

Mn(III) $S = 2$

Mn(IV) $S = 3/2$

Oxygen

Carbon

$[Mn_{12}O_{12}(CH_3COO)_{16}(H_2O)_4]\cdot 2CH_3COOH\cdot 4H_2O$

R. Sessoli et al. JACS **115**, 1804 (1993)

Well defined giant spin ($S = 10$) at low temperatures ($T < 35$ K)

- Easy-axis anisotropy due to Jahn-Teller distortion on Mn(III)
- Crystallizes into a tetragonal structure with S_4 site symmetry
- Organic ligands isolate the molecules

Quantum effects at the nanoscale ($S = 10$)

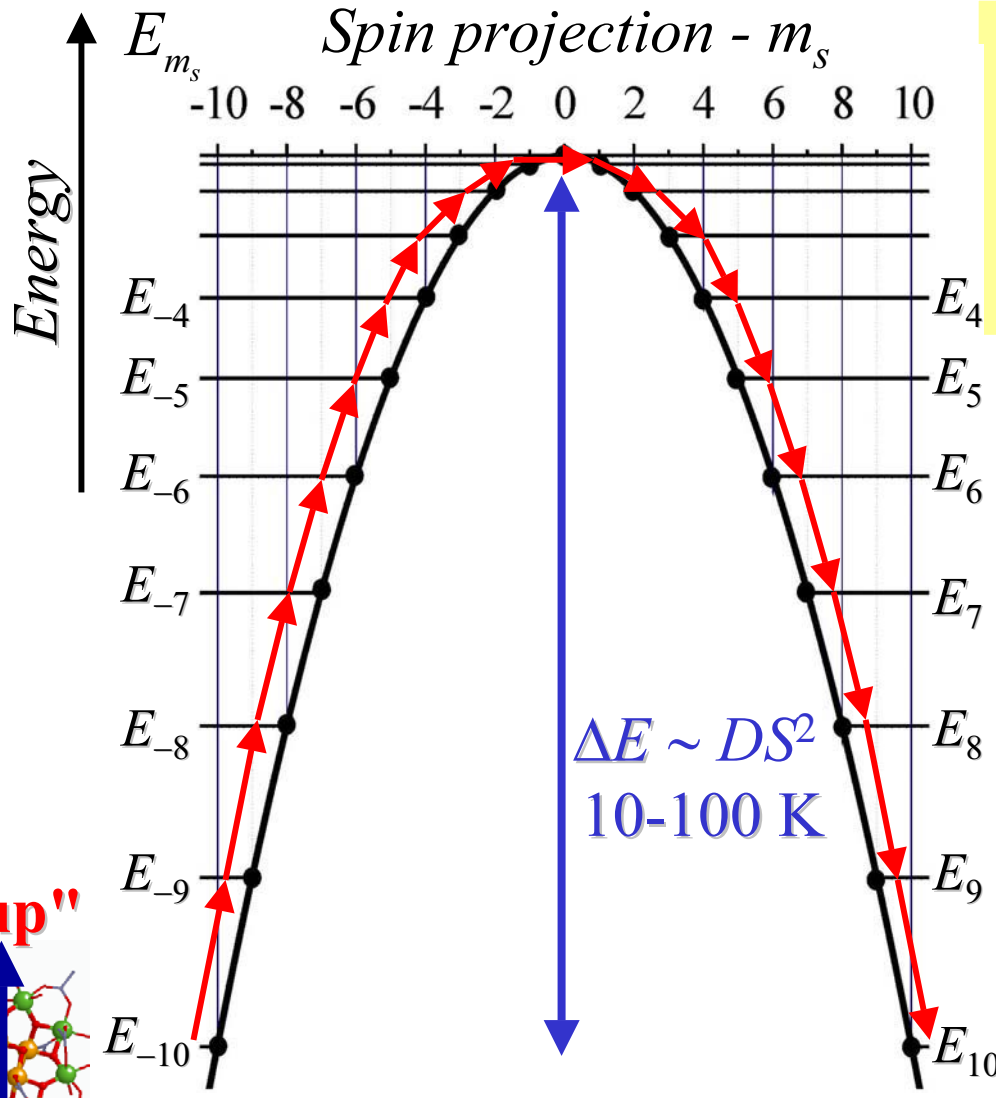

Simplest case: cylindrical (axial) z.f.s. interaction

$$\hat{\mathcal{H}} = D\hat{S}_z^2 \qquad (D < 0)$$

Eigenvalues given by:

$$\mathcal{E}(m_s) = -|D| m_s^2$$

- Small barrier - DS^2
- Superparamagnet at ordinary temperatures

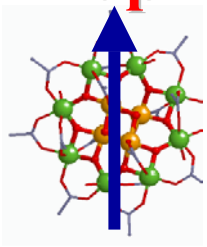

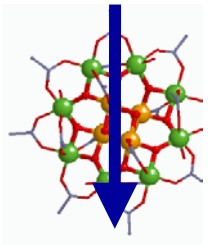

$|D| \sim 0.1 - 1$ K for a typical single molecule magnet

Quantum effects at the nanoscale ($S = 10$)

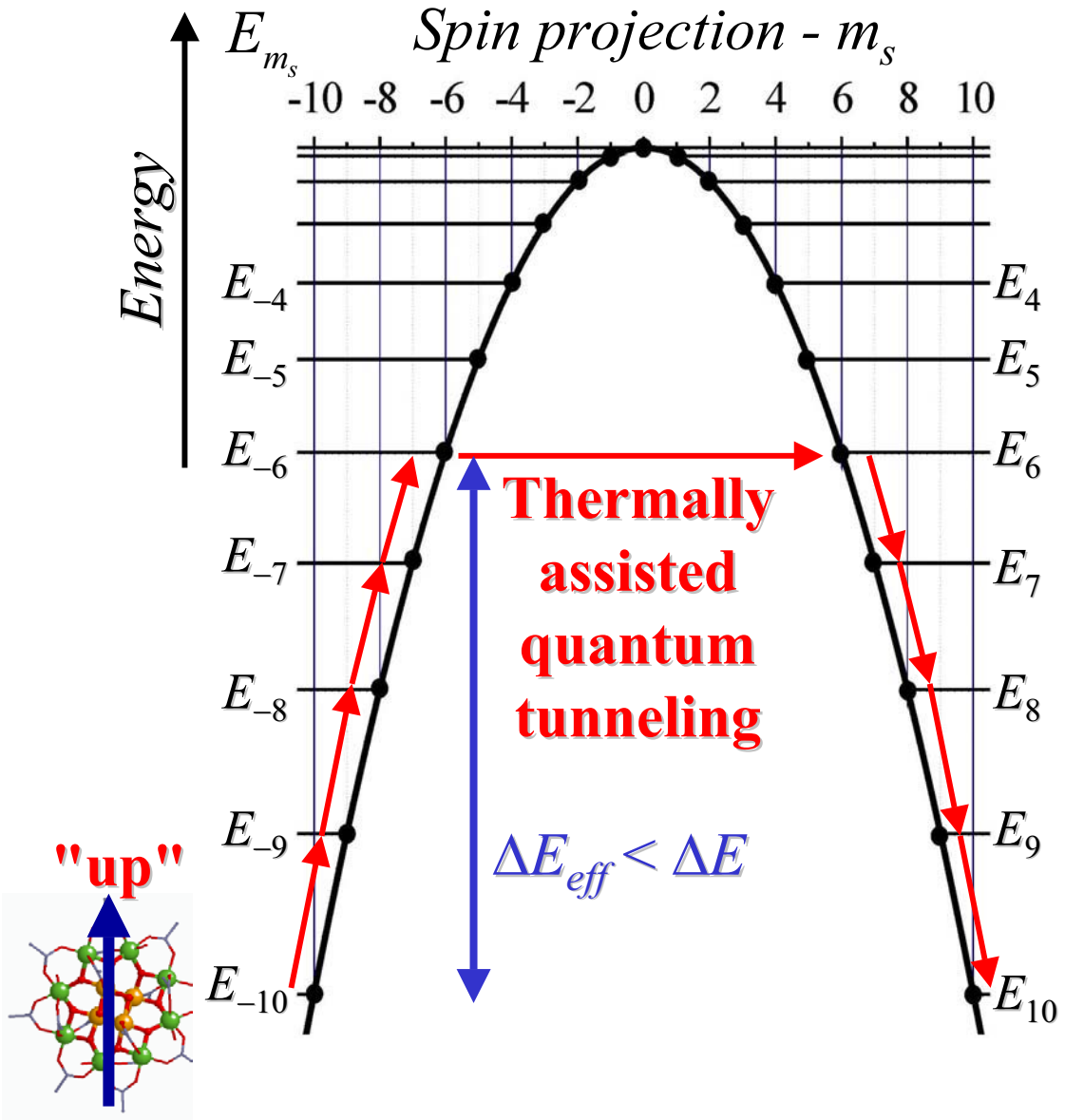

Break axial symmetry:

$$\hat{\mathcal{H}} = D\hat{S}_z^2 + \hat{\mathcal{H}}_T$$

$\mathcal{H}_T \Rightarrow$ interactions which do not commute with $\hat{S}_z$

- m_s **not** good quantum #
- Mixing of m_s states

$\Rightarrow$ resonant tunneling (of m_s) through barrier

- Lower effective barrier

Quantum effects at the nanoscale ($S = 10$)

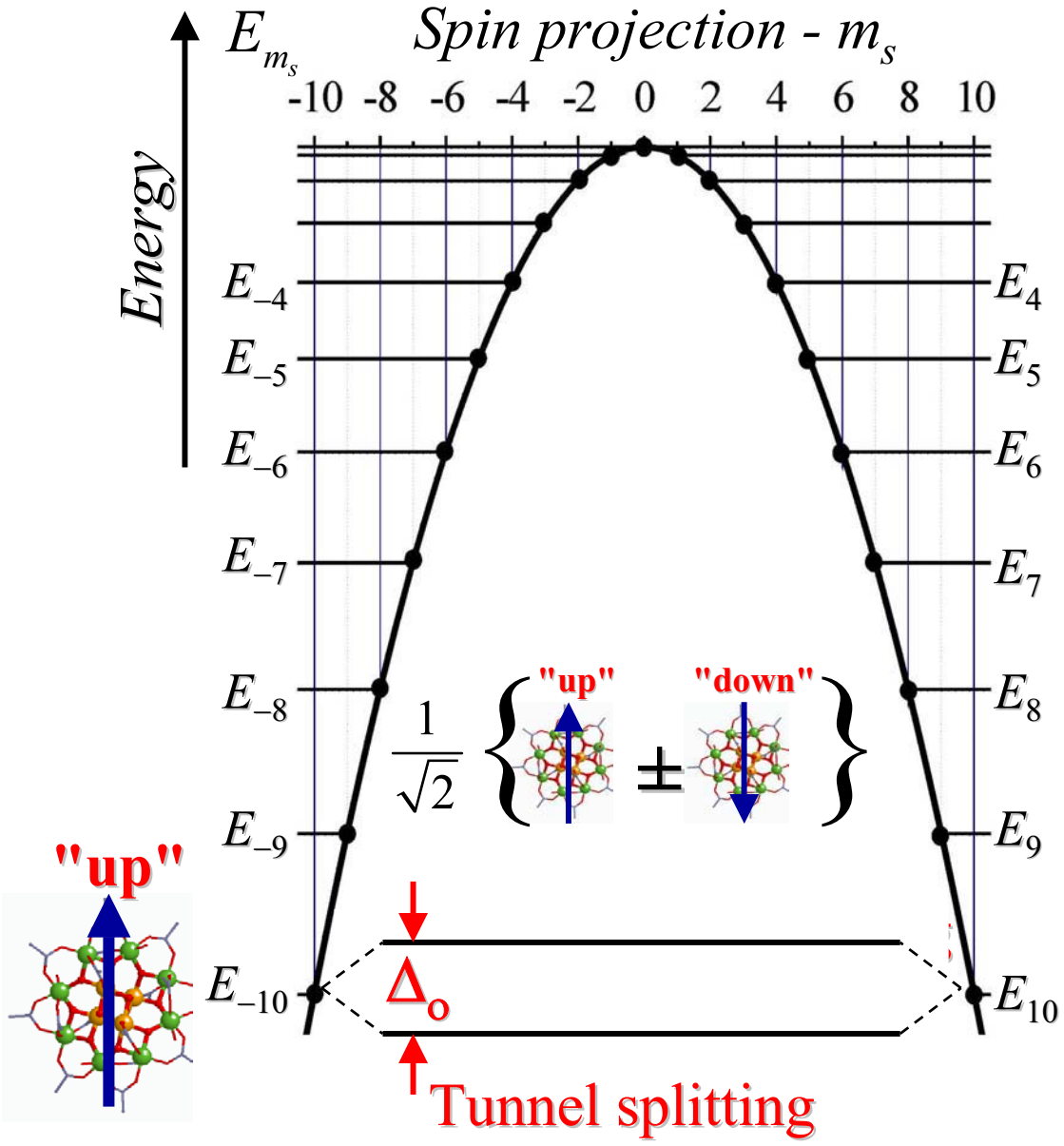

letters to nature

Quantum computing in molecular magnets

Michael N. Leuenberger & Daniel Loss

Department of Physics and Astronomy, University of Basel, Klingelbergstrasse 82, 4056 Basel, Switzerland

Shor and Grover demonstrated that a quantum computer can outperform any classical computer in factoring numbers[1] and in searching a database[2] by exploiting the parallelism of quantum mechanics. Whereas Shor's algorithm requires both superposition and entanglement of a many-particle system[3], the superposition of single-particle quantum states is sufficient for Grover's algorithm[4]. Recently, the latter has been successfully implemented[5] using Rydberg atoms. Here we propose an implementation of Grover's algorithm that uses molecular magnets[6–10], which are solid-state systems with a large spin; their spin eigenstates make them natural candidates for single-particle systems. We show theoretically that molecular magnets can be used to build dense and efficient memory devices based on the Grover algorithm. In particular, one single crystal can serve as a storage unit of a dynamic random access memory device. Fast electron spin resonance pulses can be used to decode and read out stored numbers of up to 10^5, with access times as short as 10^{-10} seconds. We show that our proposal should be feasible using the molecular magnets Fe_8 and Mn_{12}.

Mn_{12}-ac, $S = 10$

$$\hat{\mathcal{H}} = D\hat{S}_z^2 + \hat{\mathcal{H}}_T; \quad \hat{\mathcal{H}}_T = ???$$

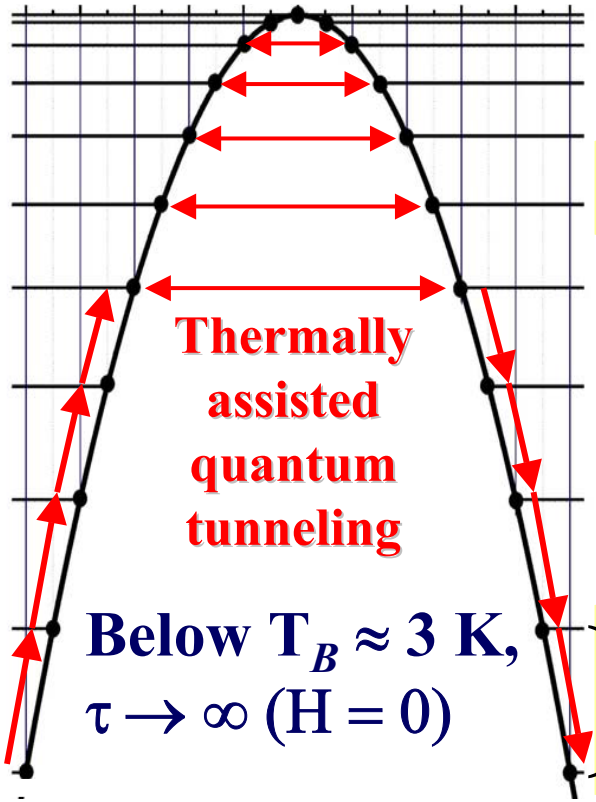

D ≈ 0.6 K

Thermally assisted quantum tunneling

Below $T_B \approx 3$ K,
$\tau \to \infty$ (H = 0)

300 GHz or 14.4 k_B

Fe_8, $S = 10$

$$\hat{\mathcal{H}} = D\hat{S}_z^2 + E\left(\hat{S}_x^2 - \hat{S}_y^2\right) + \hat{\mathcal{H}}'$$

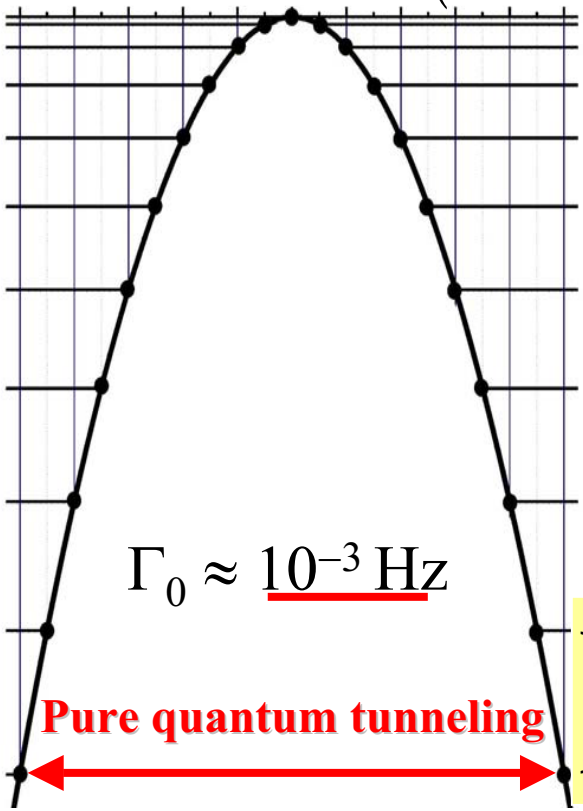

D ≈ 0.2 K

$D/E \approx 5$

$\Gamma_0 \approx 10^{-3}$ Hz

Pure quantum tunneling

115 GHz or 5.5 k_B

- Many potential sources of transverse anisotropy for Mn_{12}-ac:
  - Internal dipolar, exchange and hyperfine fields;
  - Higher order zero-field-splitting interactions;
  - Disorder, lattice defects, etc..
- However, after 10 years, the symmetry is poorly understood.

Application of a magnetic field

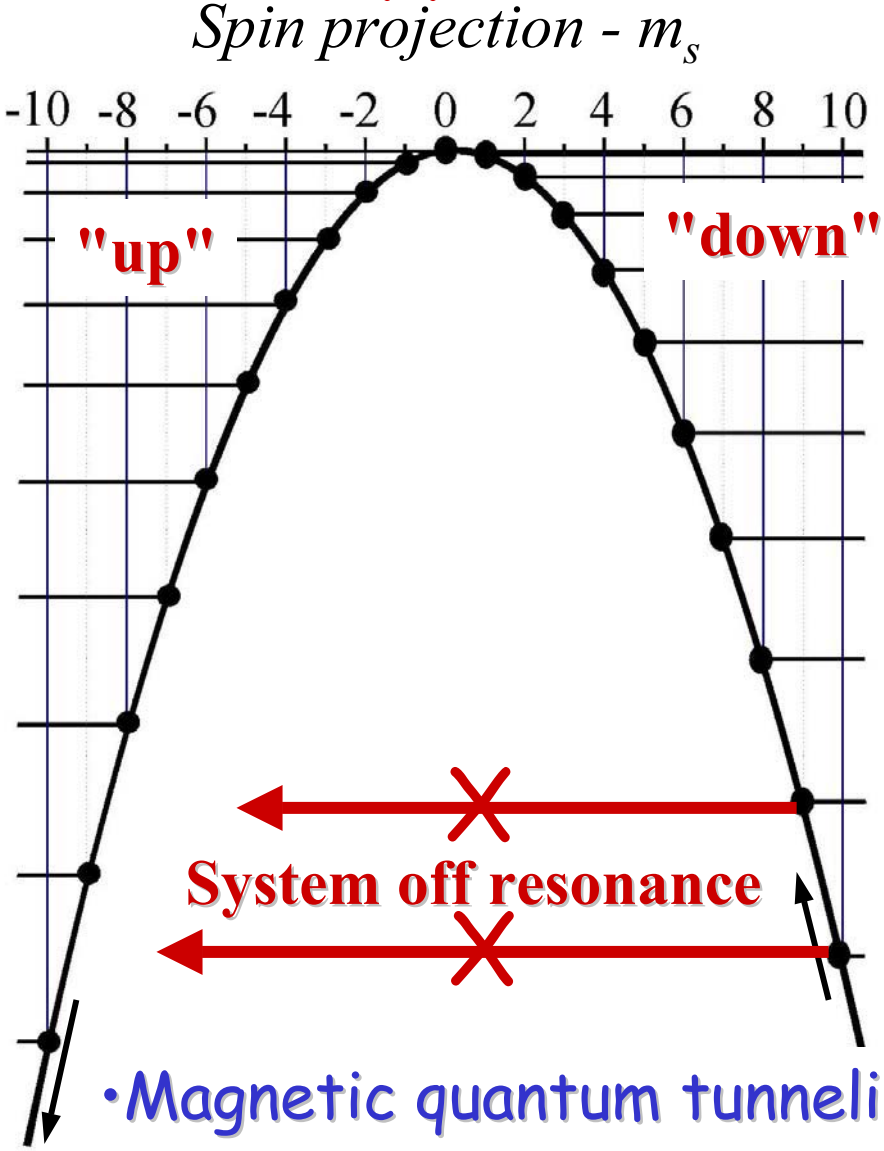

$$\hat{\mathcal{H}} = D\hat{S}_z^2 + \hat{\mathcal{H}}_T + g\mu_B \vec{B}\cdot\hat{S}$$

$$\vec{B}\cdot\hat{S} \equiv B_x\hat{S}_x + B_y\hat{S}_y + B_z\hat{S}_z$$

Several important points to note:

- Applied field represents another source of transverse anisotropy
- Zeeman interaction contains odd powers of $\hat{S}_x$ and $\hat{S}_y$

For now, consider only $B//z$:
(also neglect transverse interactions)

$$\mathcal{E}(m_s) = -|D|m_s^2 + g\mu_B B m_s$$

- Magnetic quantum tunneling is suppressed
- Metastable magnetization is blocked ("down" spins)

Application of a magnetic field

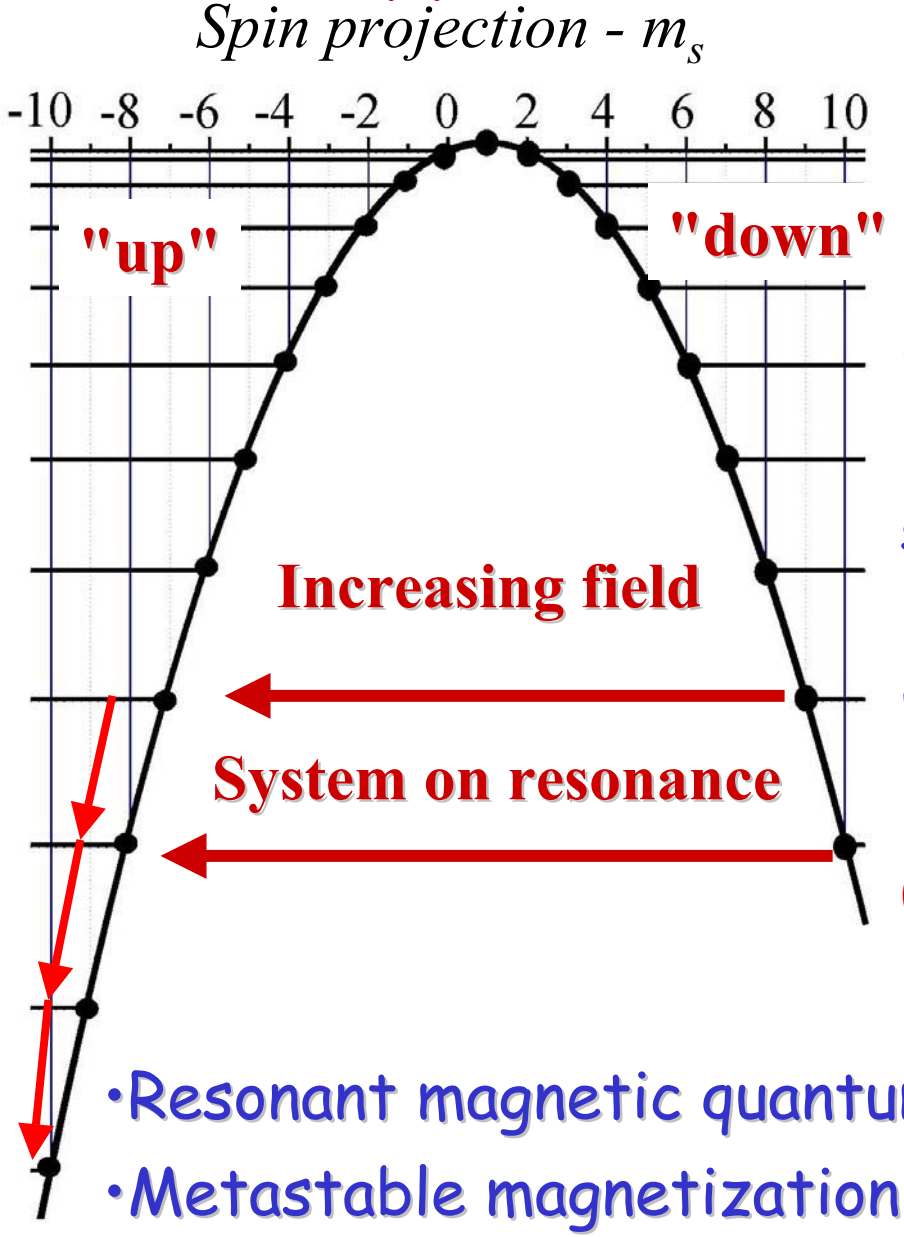

$$\hat{\mathcal{H}} = D\hat{S}_z^2 + \hat{\mathcal{H}}_T + g\mu_B \vec{B}\cdot\hat{S}$$

$$\vec{B}\cdot\hat{S} \equiv B_x\hat{S}_x + B_y\hat{S}_y + B_z\hat{S}_z$$

Several important points to note:

- Applied field represents another source of transverse anisotropy.
- Zeeman interaction contains odd powers of $\hat{S}_x$ and $\hat{S}_y$.

For now, consider only $B//z$:
(also neglect transverse interactions)

$$\mathcal{E}(m_s) = -|D|m_s^2 + g\mu_B B m_s$$

- Resonant magnetic quantum tunneling resumes
- Metastable magnetization can relax from "down" to "up"

Hysteresis and magnetization steps

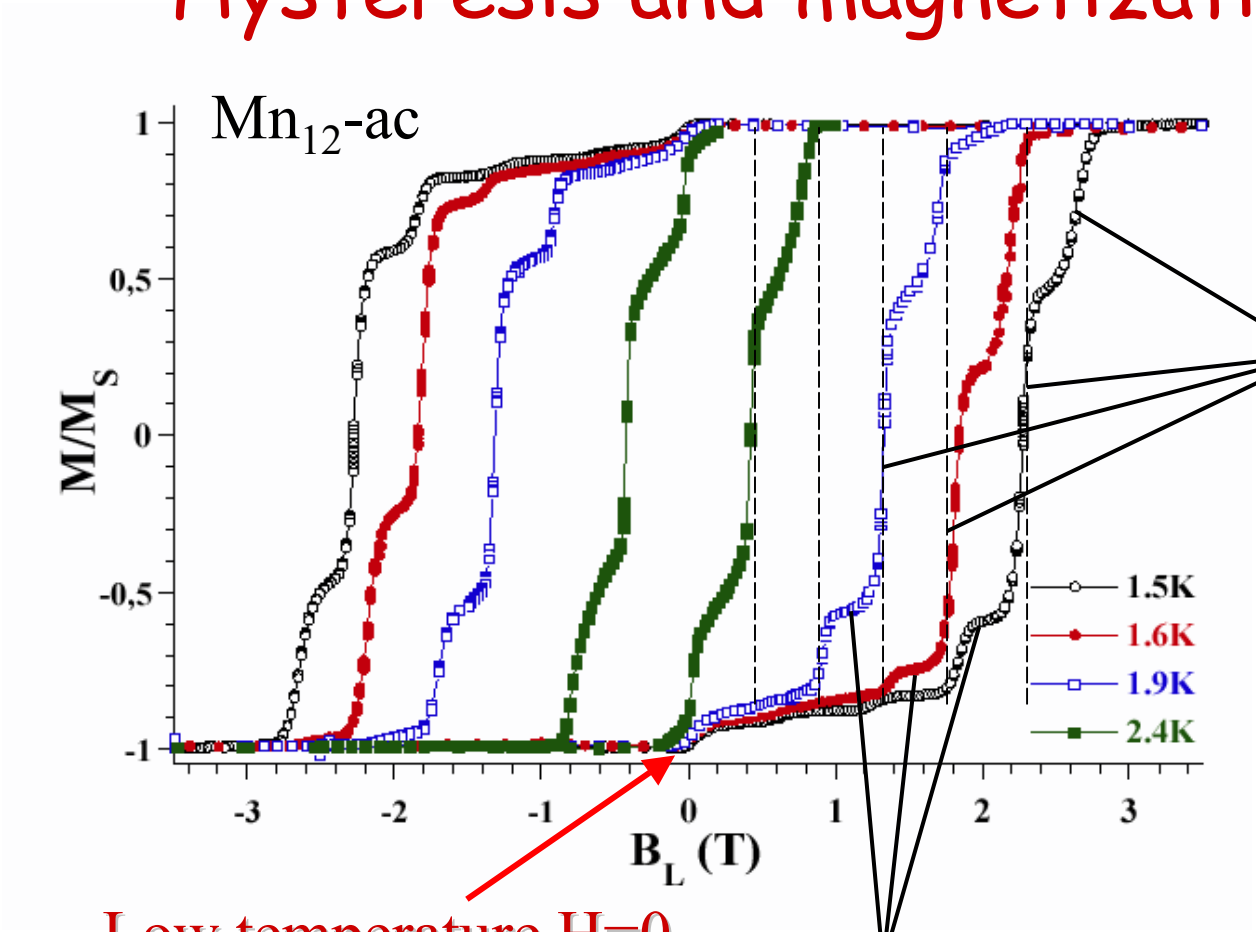

This loop represents an ensemble average of the response of many molecules

- **Friedman, Sarachik, Tejada, Ziolo, PRL (1996)**
- **Thomas, Lionti, Ballou, Gatteschi, Sessoli, Barbara, Nature (1996)**

Single-crystal, high-field/frequency EPR

$$\mathcal{E}(m_s) = -|D| m_s^2 + g\mu_B B m_s$$

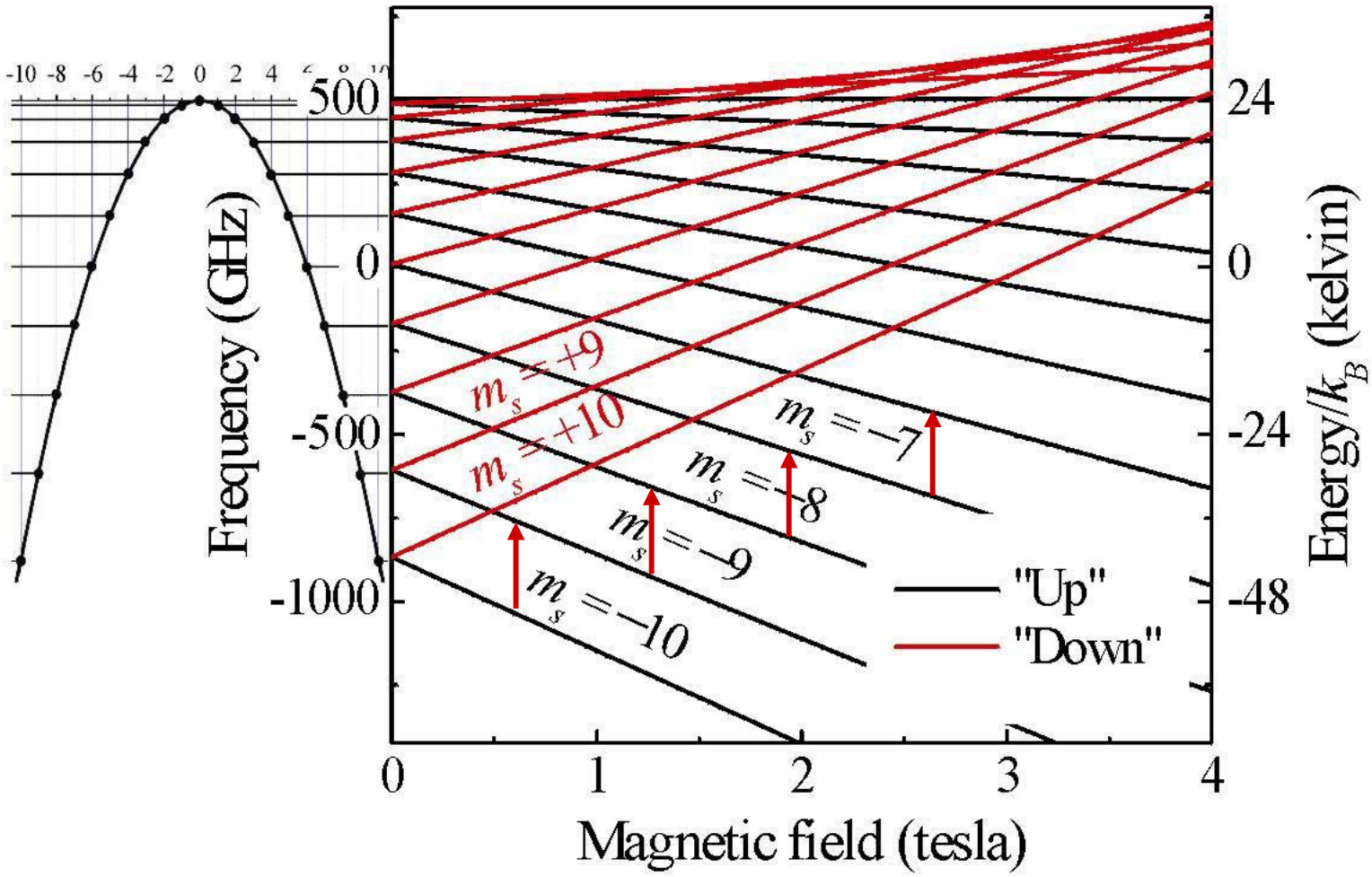

field//*z*

z, S_4-axis

H_z

- Magnetic dipole transitions ($\Delta m_s = \pm 1$) - note frequency scale!

Experimental Technique

- ***Frequency Range***: 8-800 GHz
  - *Millimeter-wave vector network analyzer*
  - *Superheterodyne detection*
  - *Association with various sources/detectors*
    - *YIG (8-18 GHz) + Schottky (up to nearly 300 GHz)*
    - *Gunn (70-102 GHz) + Schottky (up to 800 GHz)*
  - *Cavity perturbation up to nearly 400 GHz*
- ***Cryogenics system***:
  - *^{4}He variable flow (1.3 to 400 K)*
  - *^{3}He single shot (down to 0.5 K)*
  - *^{3}He/^{4}He planned (down to 0.05 K)*
- ***Magnet Systems***:
  - *Axial Magnets*
    - *Oxford Instruments (17 tesla)*
    - *NHMFL (45 tesla)*
  - *Transverse Magnet*
    - *QD PPMS (7 tesla)*
- ***Angle Control***:
  - *Transverse Magnet.*
  - *Rotating Cavity*

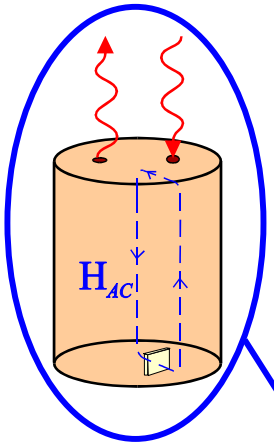

1), 2) Magnetic Field for Axial Magnet (Oxford 17 T, NHMFL 45 T)

3) Magnetic Field for Split Coil Magnet (QD PPMS 7 T)

Rotating Cavity

- **TE011 = 52 GHz (up to 400 GHz)**
  (Diameter × Height = 0.3" × 0.3")
- ***Q*** **~ 25,000 (TE011, 4.2 K)**
- **45-320 GHz**
- **Resolution < ±0.2° (< ±0.1° PPMS)**

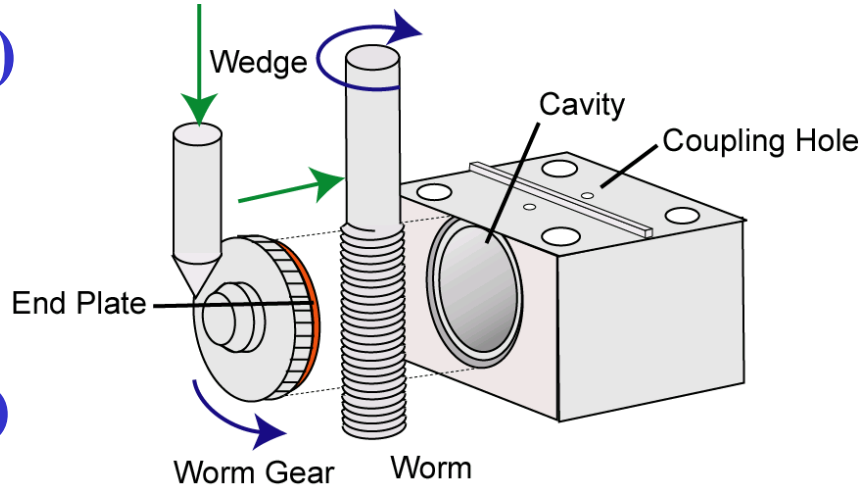

1st Generation:
25 tesla, ^{4}He system

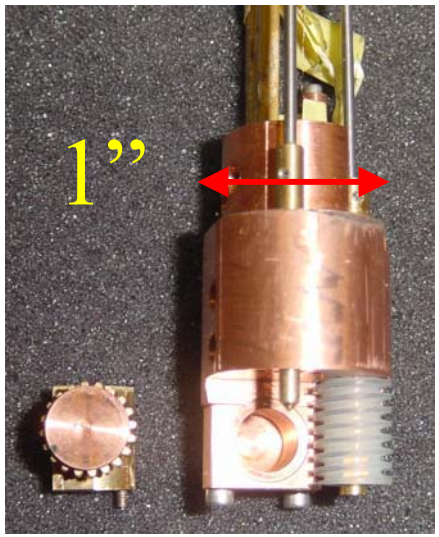

2nd Generation:
45 tesla, ^{3}He system

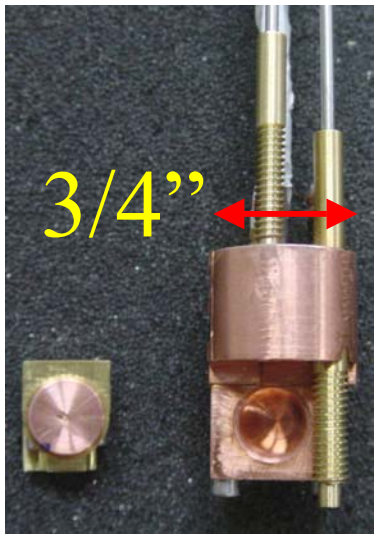

1 Axis Rotation

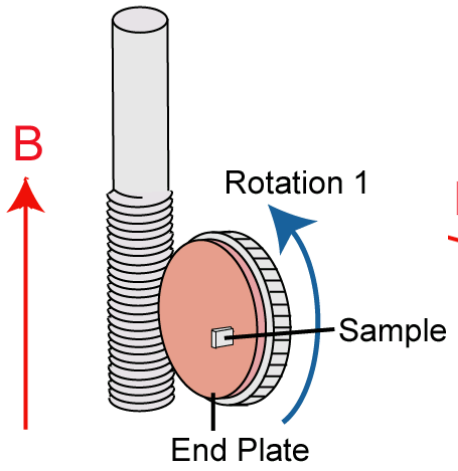

2 Axis Rotation

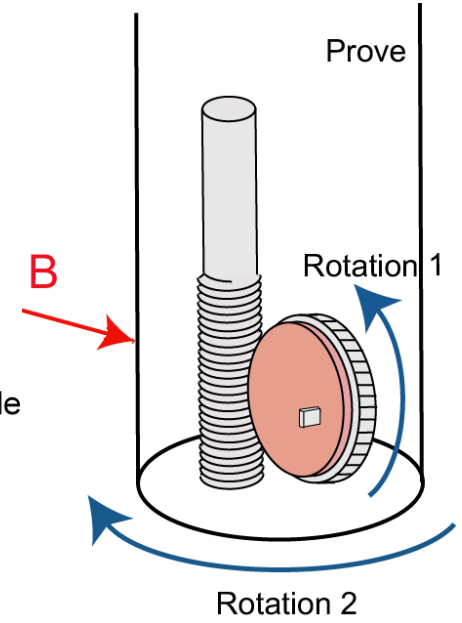

M. Mola *et al.*, Rev. Sci. Inst. **71**, 186 (2000).
S. Takahashi *et al.*, Rev. Sci. Inst. **76**, 023114 (2005).

Extended frequency coverage (2003)
Quasi-optical setup at University of Florida
continuous coverage from 170 - 715 GHz

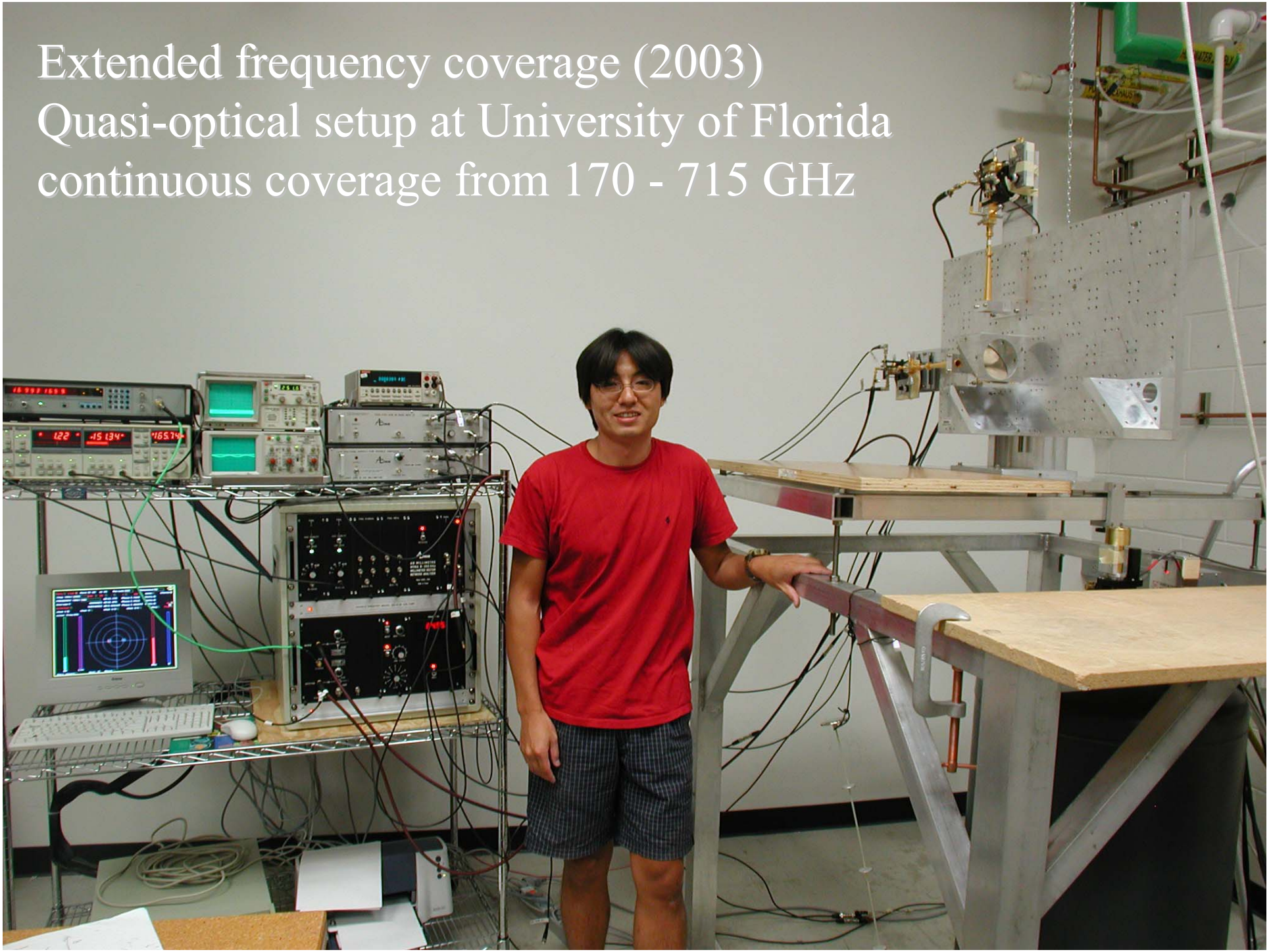

Variety in instrumentation and methodology

EPR in DC magnetic fields

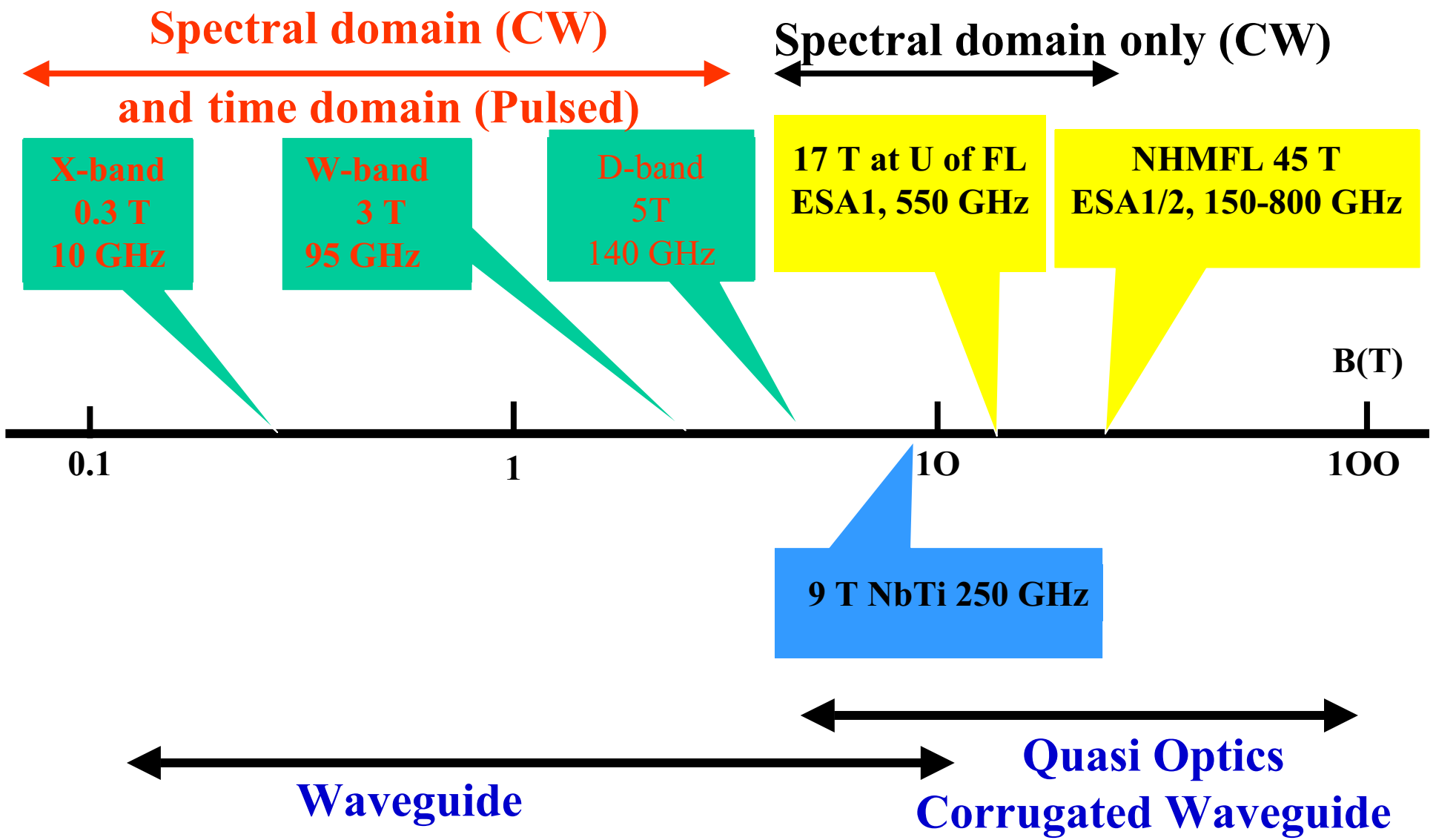

High-field sub-millimeter-wave spectroscopy at NHMFL

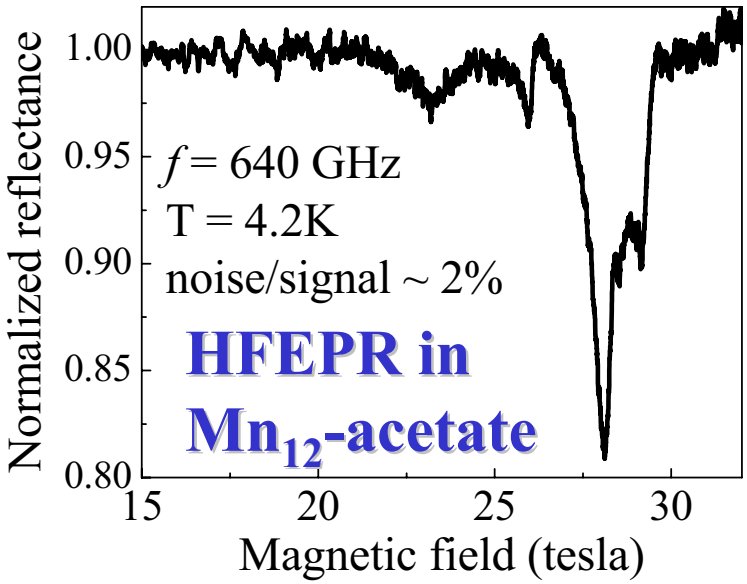

Low-loss quasi-optics
Corrugated waveguide
Solid-state electronics
f = 50 – 800 GHz (in 45 T)
Sample rotation (50-200 GHz)

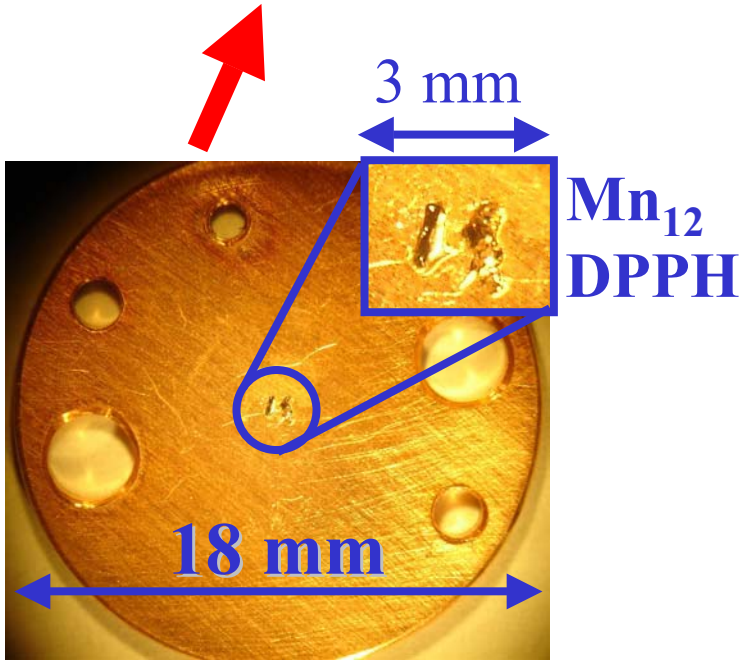

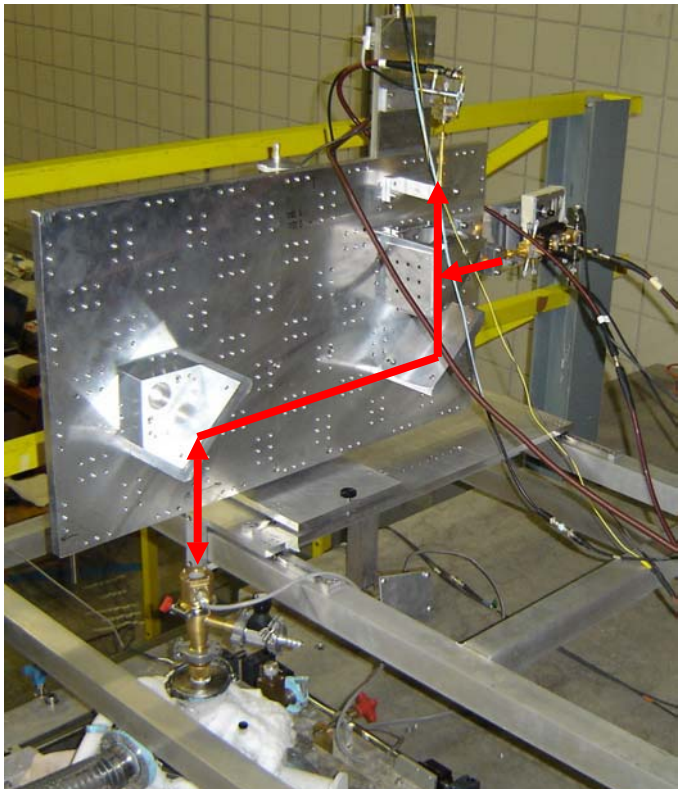

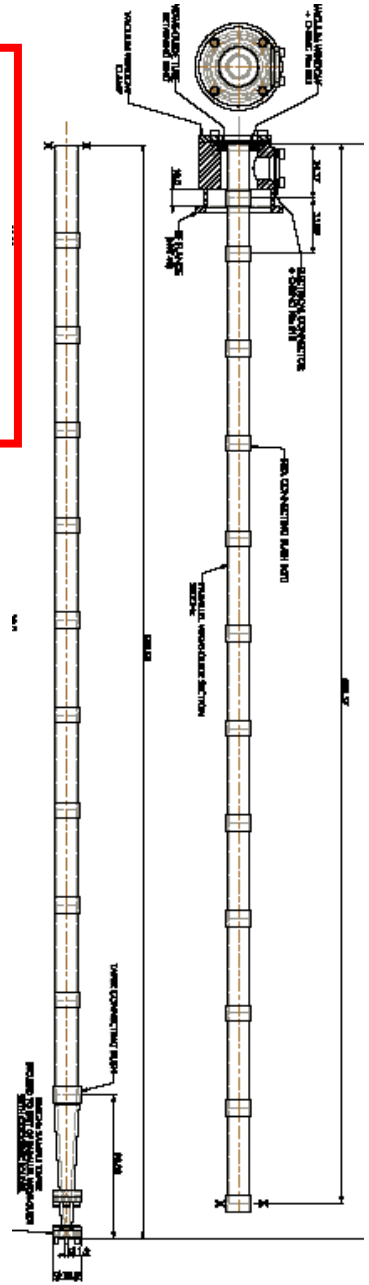

NHMFL (Gainesville & Tallahassee) EPR
A Unique Multi-Frequency and High-Field Facility

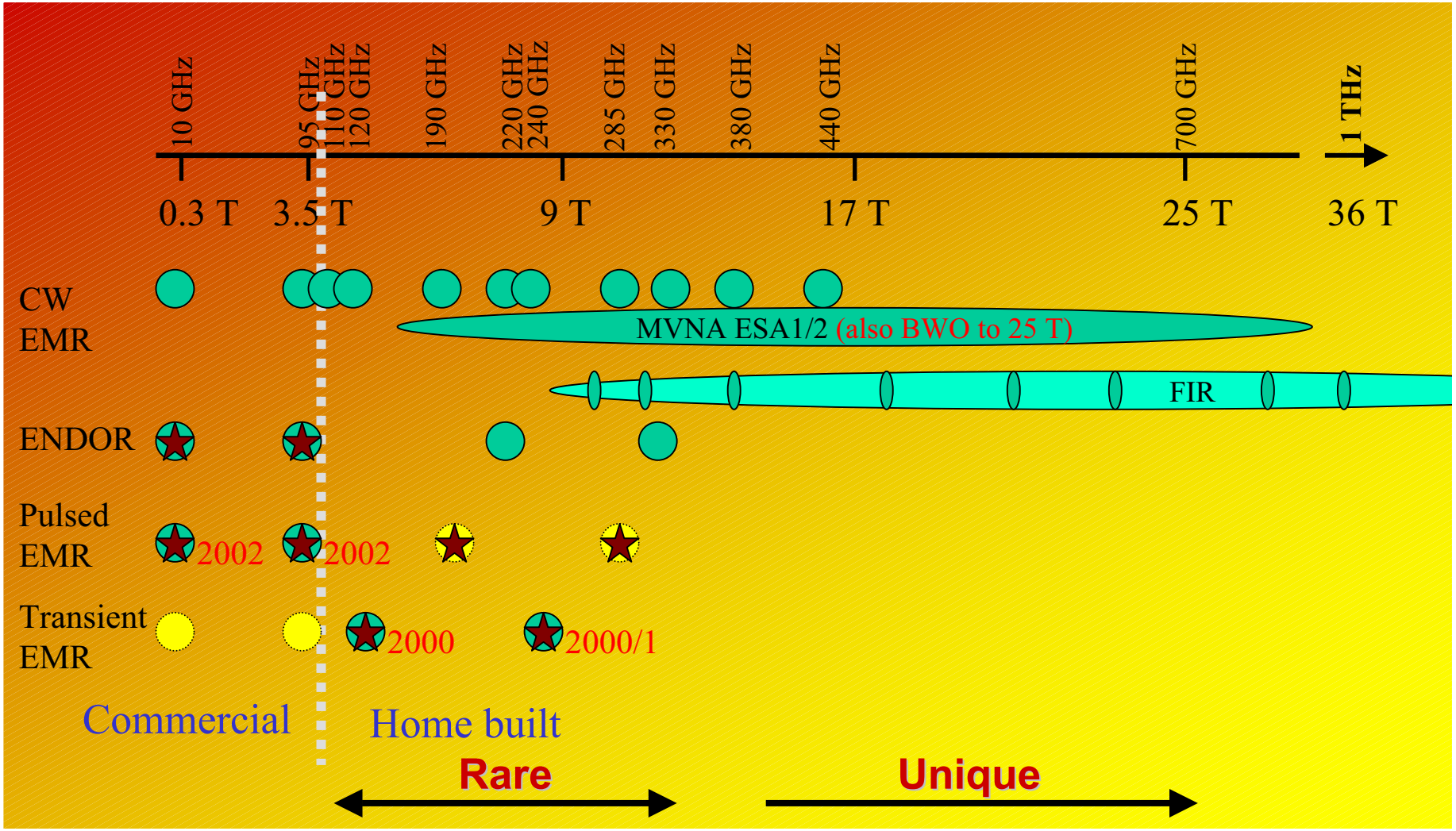

Specifications...

Max resistive field: 33.1 T

NHMFL

- **Two 20 MW supplies**
  V_m = 500 V; I_m = 20 kA
- **Ripple < 10ppm**
- **33/30 T, 32mm bore**
- **25 T, 52mm**
- **20 T, 200mm**
- **T ≈ 35mK to >RT**
- **Optics, magnetometry, transport, *etc*..**

- World record magnet
  - **33.1 tesla @ 38 kA**
  - **19 MW!!**
  - **Water - 140 Lit/s**
    ΔT=35°C (≈ 19 MW)

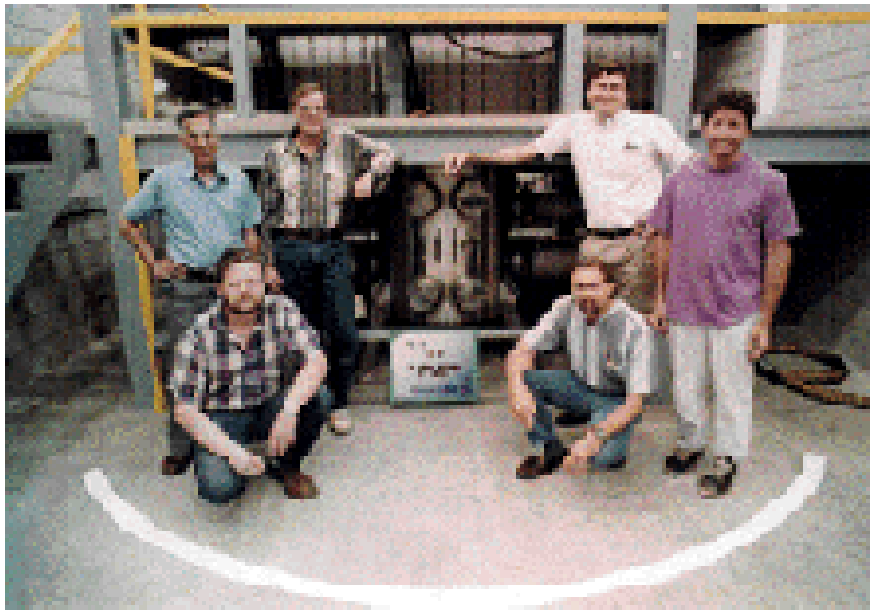

Max field: 45 T (superconducting hybrid)

Original driving force behind these techniques: Fermi surface spectroscopy of low-D superconductors

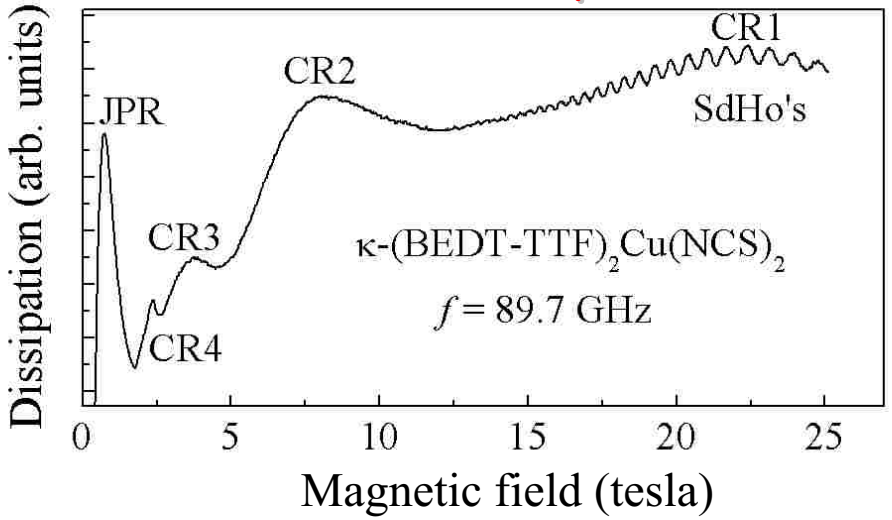

S. Hill, PRB **55**, 4931 (1997)
S. Hill et al., PRL **84**, 3374 (2000)
S. Hill et al., PRL **86**, 2130 (2001)
S. Hill et al., PRL **86**, 3451 (2001)
Kovalev et al., PRB **66**, 134513 (2002)
Kovalev et al., PRL **91**, 216402 (2003)

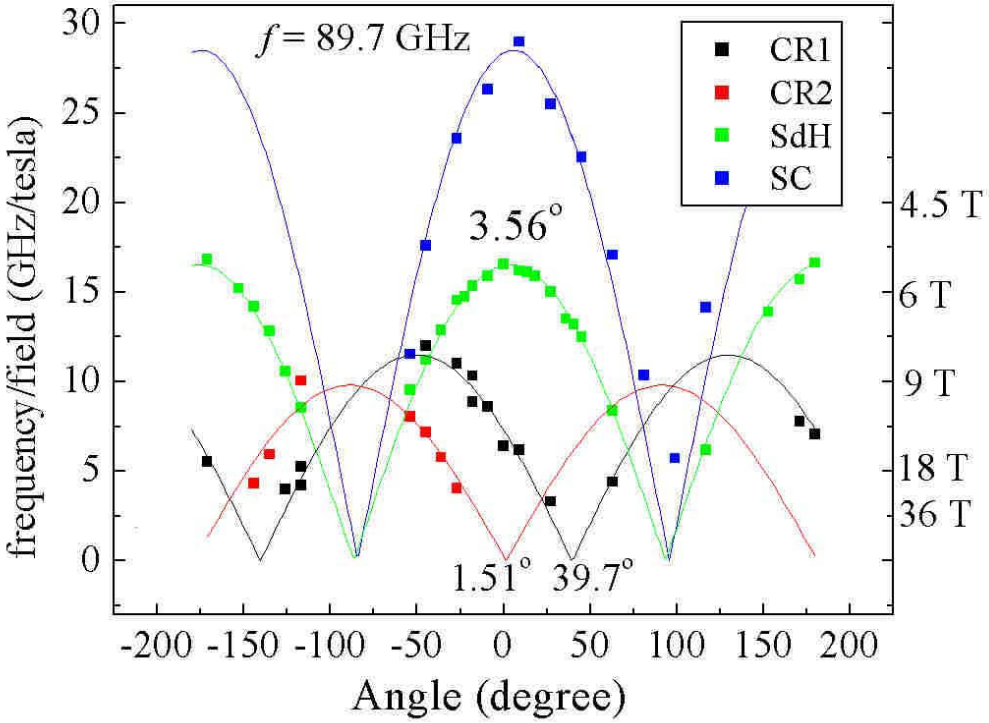

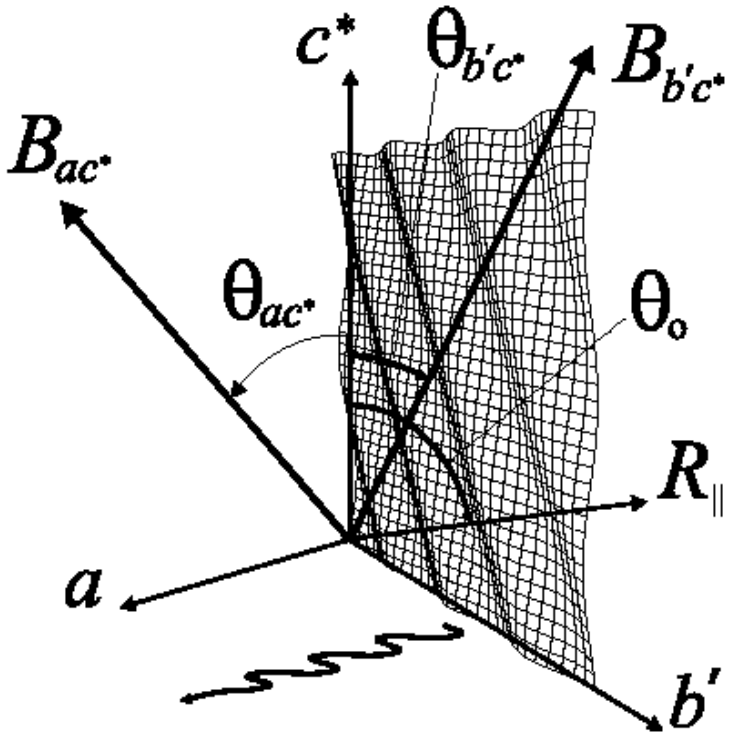

Symmetry of quantum tunneling in various Mn_{12} complexes

Single-crystal, high-field/frequency EPR

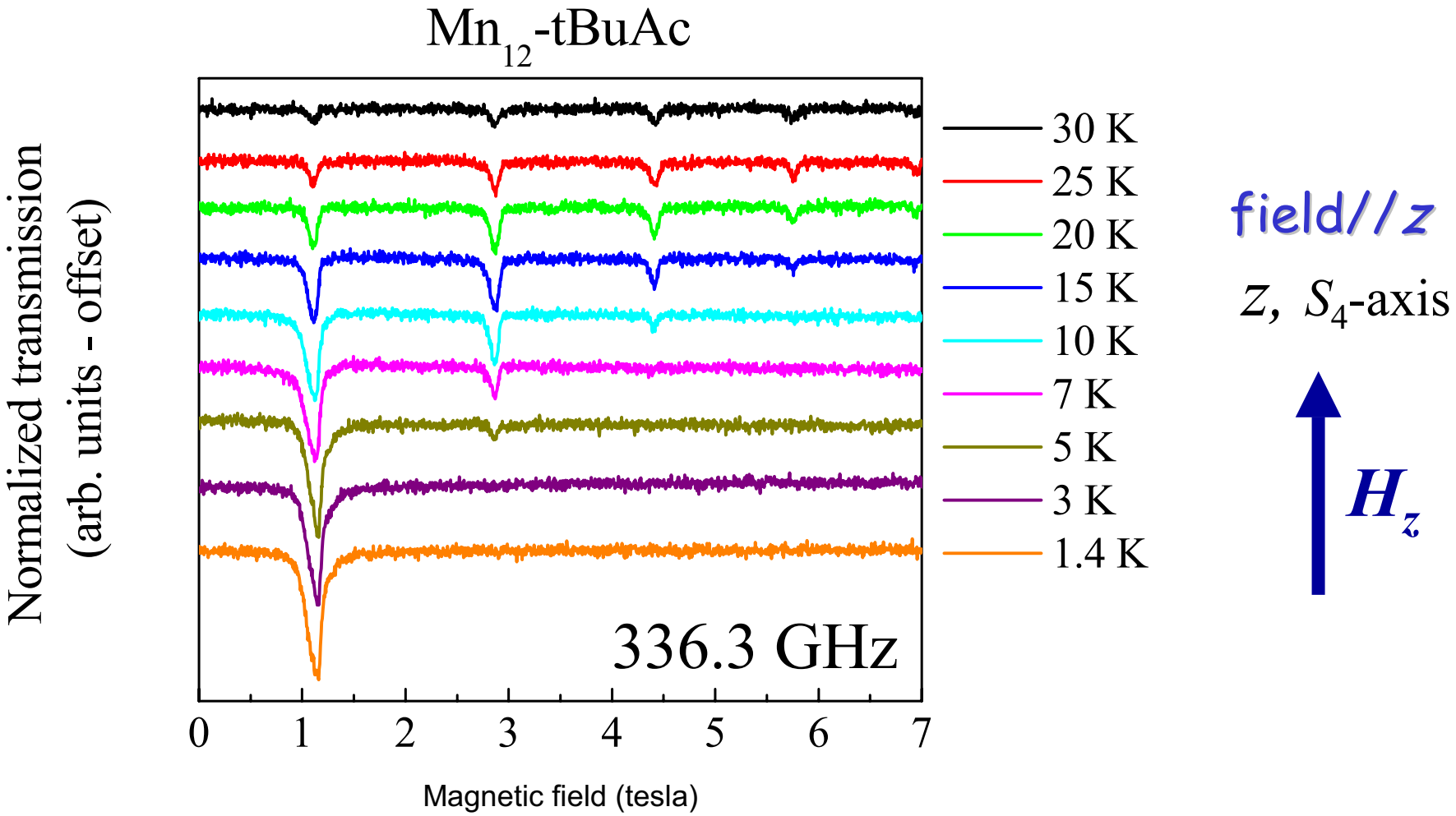

- First of all, these terms are not so small:

$$\hat{\mathcal{H}} = \left(\frac{D'}{S^2}\right)\hat{S}_z^2 + \left(\frac{B'}{S^4}\right)\hat{S}_z^4 + \left(\frac{C'}{S^4}\right)\hat{O}_4^4$$

$$D' = 55\,\mathrm{K}; \qquad B' = 13\,\mathrm{K}; \qquad C' = 0.3\,\mathrm{K}$$

Single-crystal, high-field/frequency EPR

Rotate field in *xy*-plane and look for symmetry effects

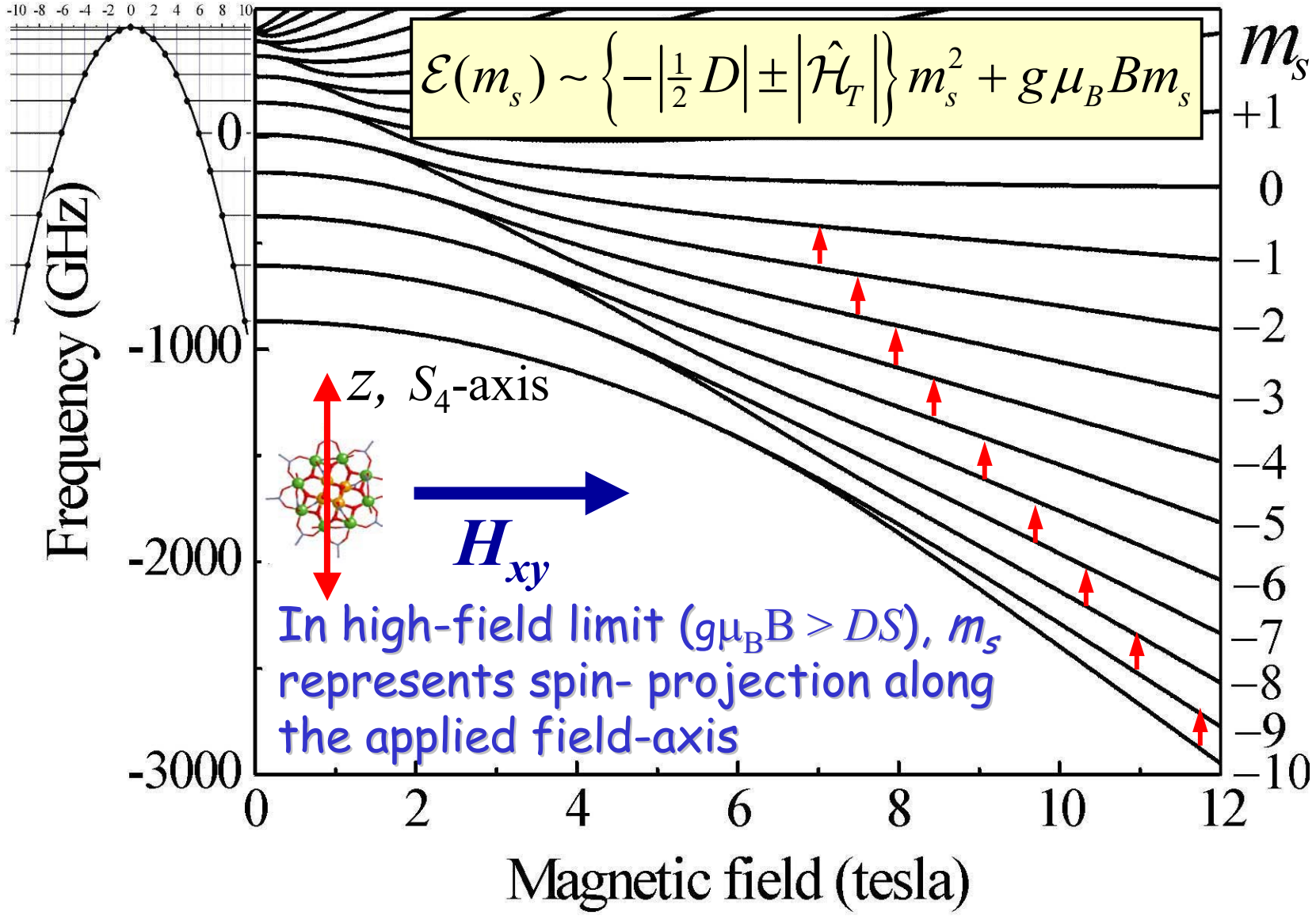

Hard-plane rotations for *d*-Mn_{12}-acetate

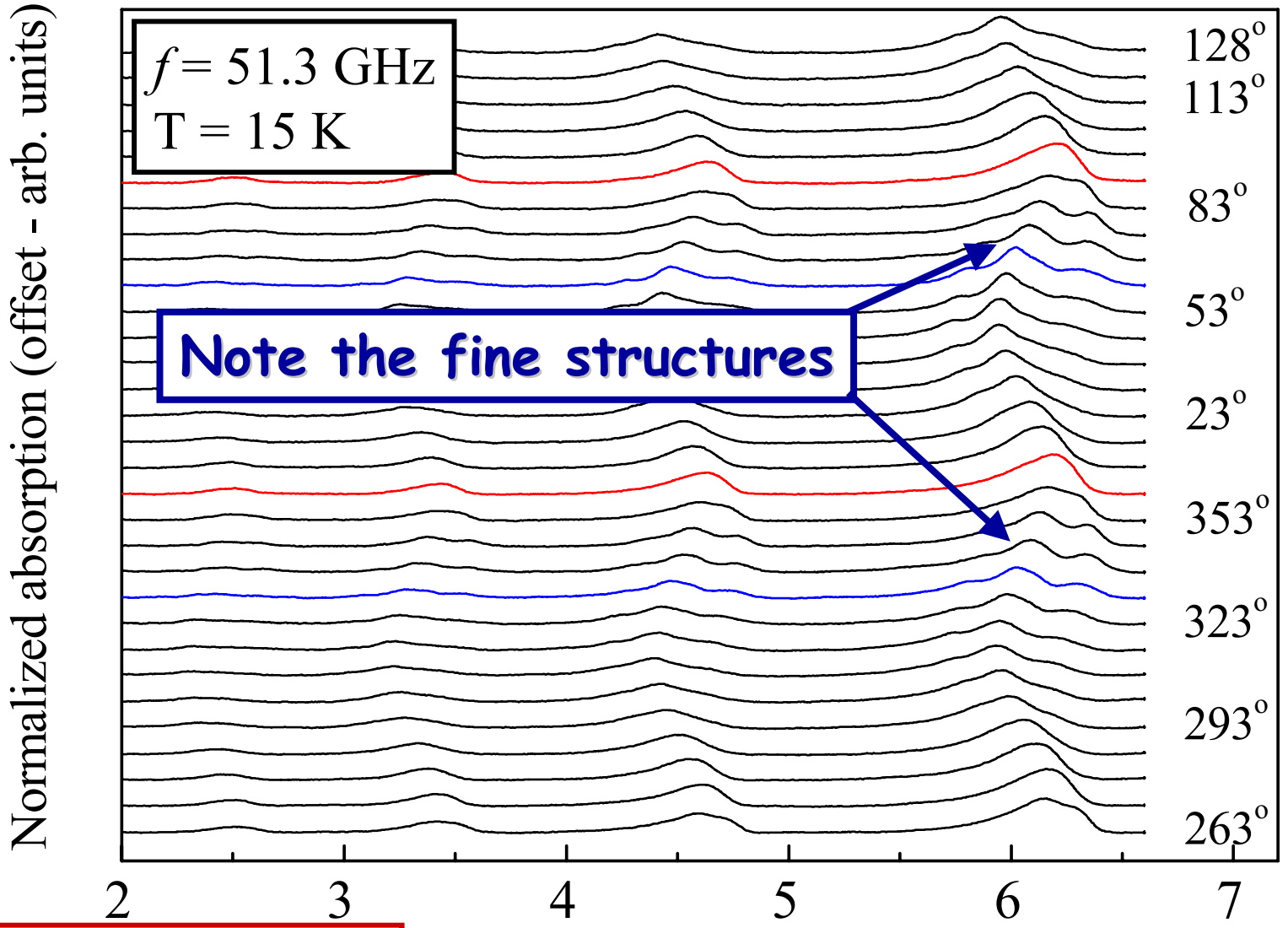

arXiv/cond-mat/0404390

Data for *h*-Mn_{12}-acetate in: S. Hill et al., PRL **90,** 217204 (2003)

Determination of transverse crystal-field interactions in d-Mn_{12}-Ac

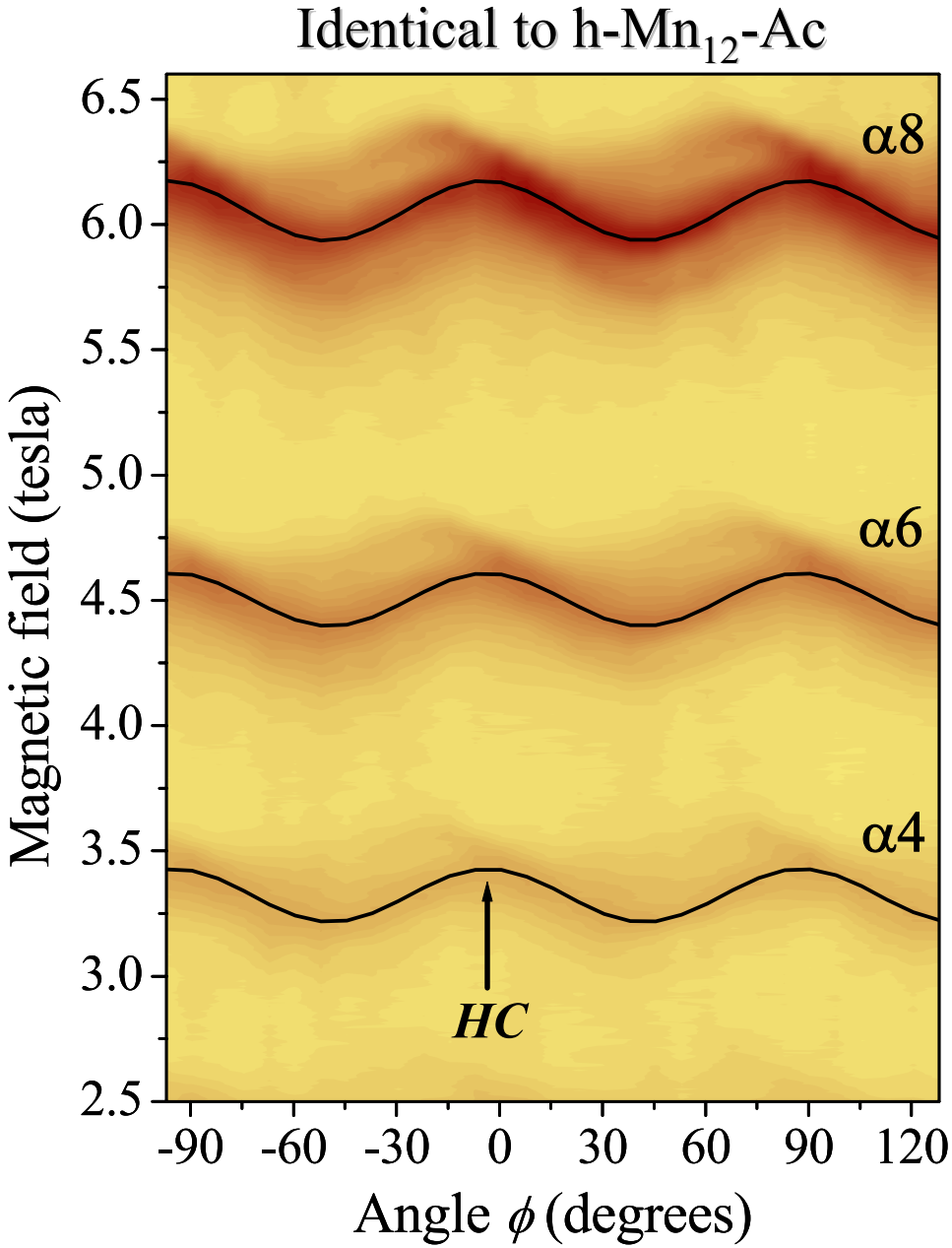

Hard-plane (*xy*-plane) rotations

- Four-fold line shifts due to a quartic transverse interaction in $\mathcal{H}_T$
- Previously inferred from neutron studies

Mirebeau et al., PRL **83,** 628 (1999)

- B_4^4 is the only free parameter in our fit

S. Hill et al., PRL **90,** 217204 (2003)

$$\tfrac{1}{2} B_4^4 \left(\hat{S}_+^4 + \hat{S}_-^4 \right)$$

$$B_4^4 = 46(1)\,\mu\mathrm{K}$$

Determination of transverse crystal-field interactions in d-Mn_{12}-Ac

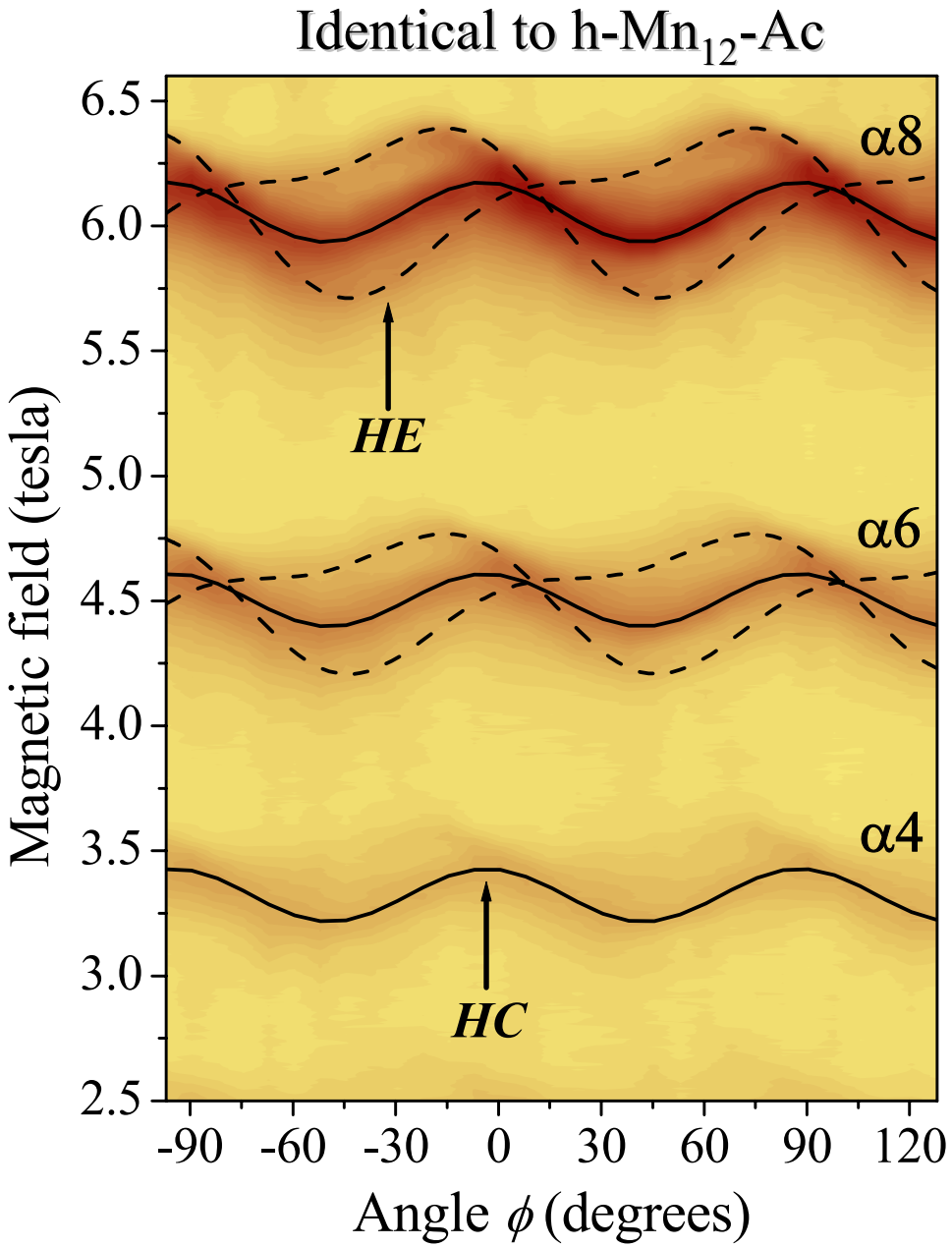

- Two-fold line shifts associated with the high- and low-field shoulders due to a quadratic transverse interaction in $\mathcal{H}_T$

del Barco et al., arXiv/cond-mat/0404390

$$E\left(\hat{S}_x^2 - \hat{S}_y^2\right)$$

$$E \approx 20\,\mathrm{mK}$$

Incompatible with the crystallographic symmetry!

***HC* and *HE* incommensurate!**

Disorder lowers the symmetry of the molecules

$$\mathcal{H} = -DS_z^2 - BS_z^4 - g\mu_B H S_z \cos\theta + \mathcal{H}_T + \mathcal{H}_A + \mathcal{H}'$$

$$\mathcal{H}_T = -g\mu_B H_T (S_x cos\phi + S_y sin\phi)$$

$$\mathcal{H}_A = E(e_1(S_x^2 - S_y^2) + e_2(S_x \cdot S_y + S_y \cdot S_x)) + C(S_+^4 + S_-^4)$$

$$e_1 = (cos^2\beta - sin^2\beta) \quad e_2 = 2cos\beta sin\beta$$

del Barco et al., arXiv/cond-mat/0404390

$$-E(S_x^2 - S_y^2) \; + \; +E(S_x^2 - S_y^2)$$

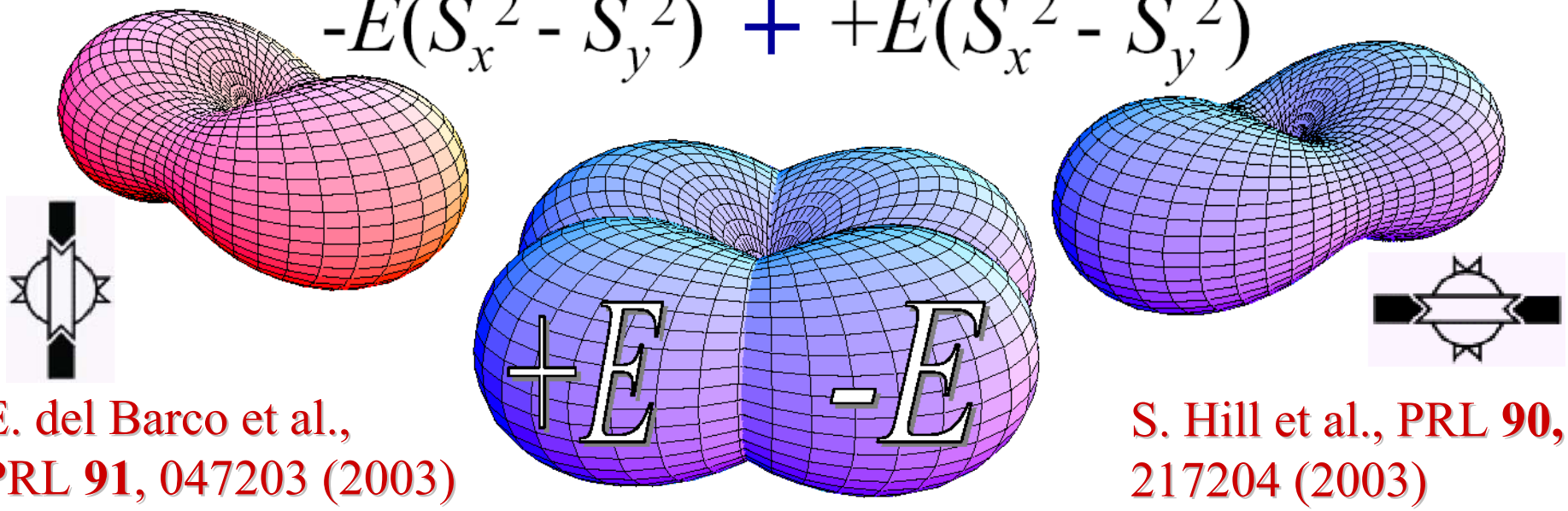

E. del Barco et al., PRL **91**, 047203 (2003)

S. Hill et al., PRL **90**, 217204 (2003)

$[Mn_{12}O_{12}(O_2CMe)_{16}(H_2O)_4]\cdot 2MeCO_2H\cdot 4H_2O$ *vs.* $[Mn_{12}O_{12}(O_2CCH_2Bu^t)_{16}(MeOH)_4]\cdot$MeOH

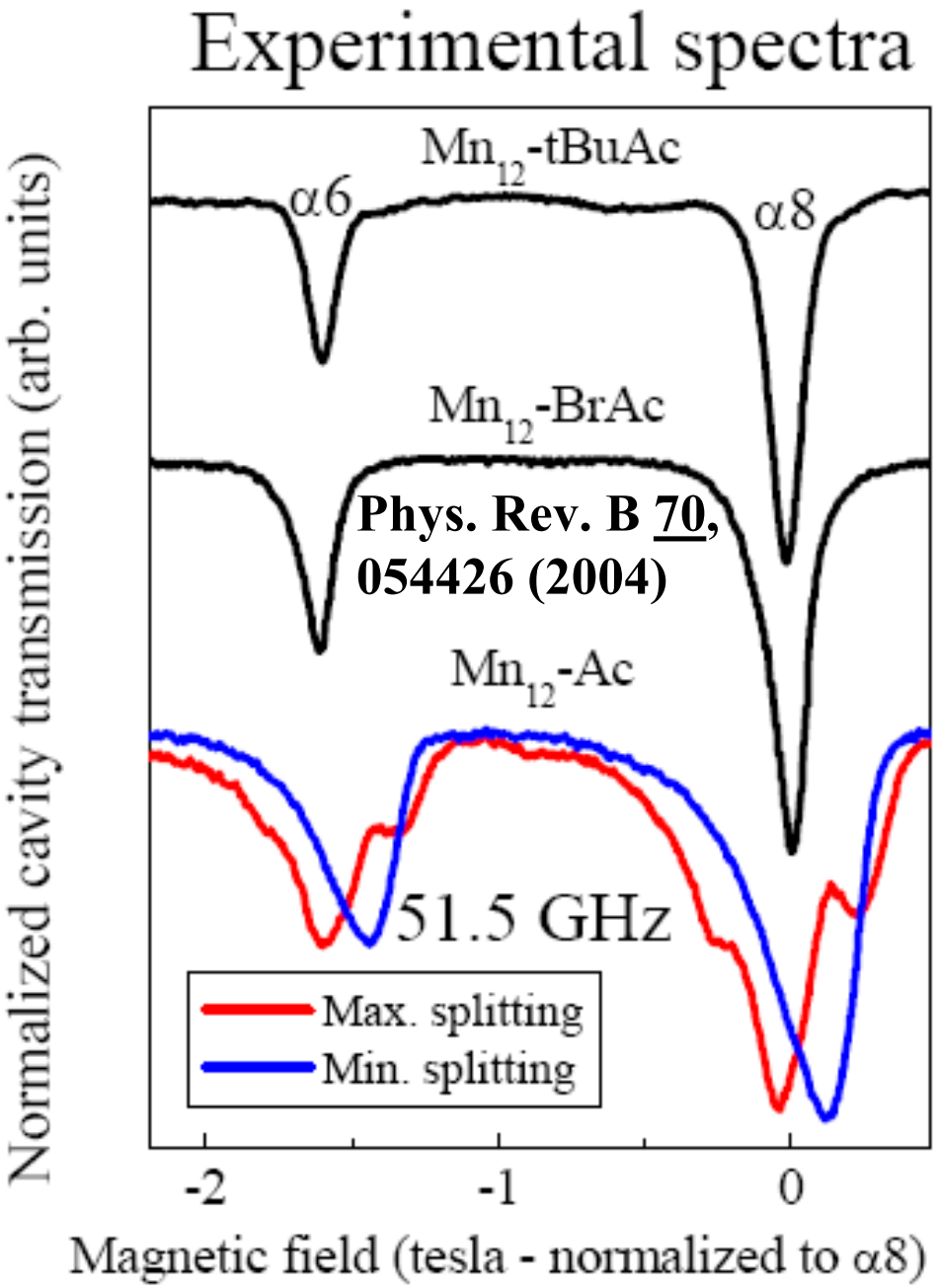

$\rightarrow [Mn_{12}O_{12}(O_2CR)_{16}(H_2O)_4] + 16\ MeCO_2H$

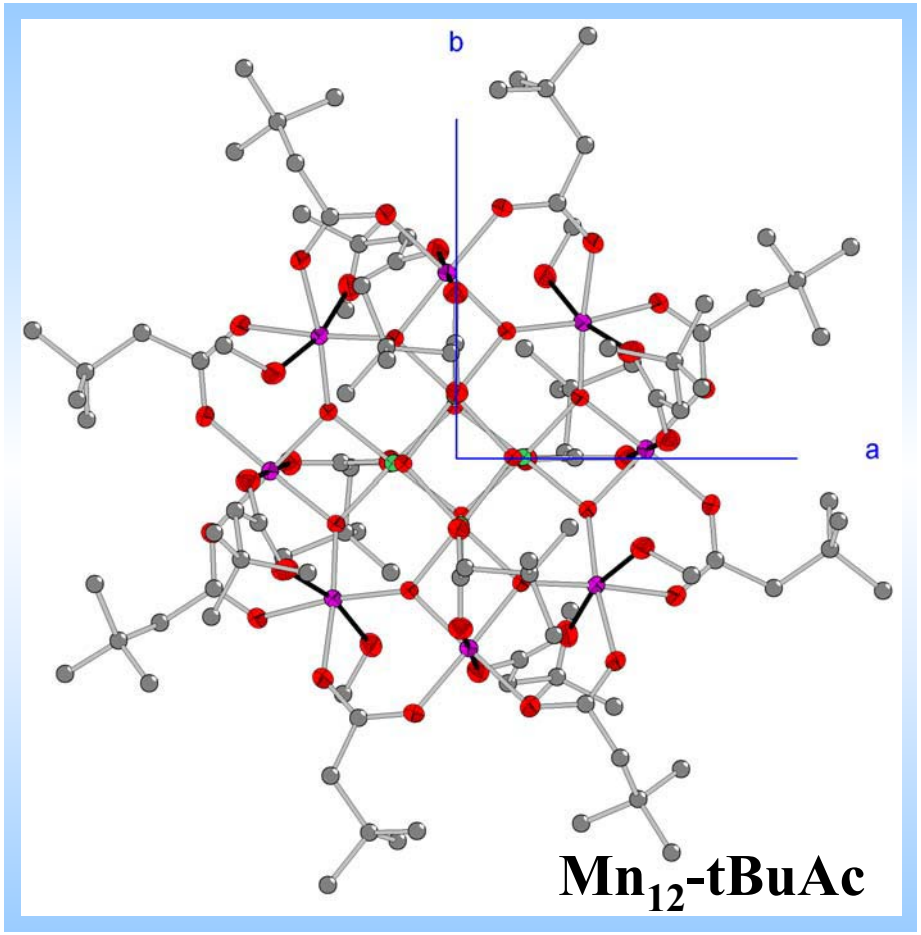

- **Less solvent of crystallization**
- **Bulky R group: well separated molecules**
- **Well aligned**

Spin Hamiltonian parameters for Mn_{12}-tBuAc

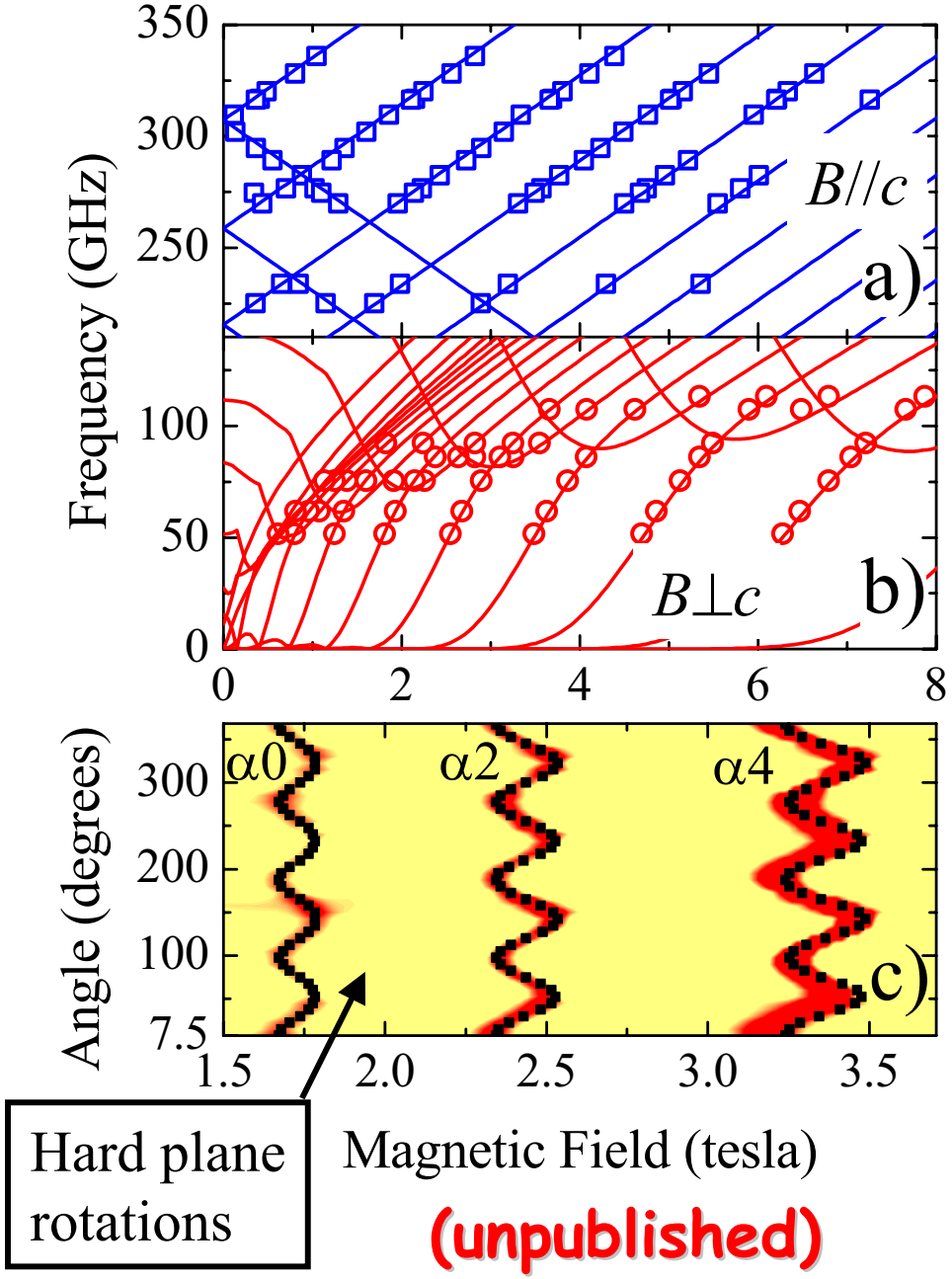

(unpublished)

Spectroscopists Hamiltonian:

$$\hat{H} = D\hat{S}_z^2 + B_4^0\hat{O}_4^0 + B_4^4\hat{O}_4^4$$

	(cm^{-1})	(kelvin)
D	$-0.462(2)$	$0.665(3)$
B_4^0	$-2.5(2)\times10^{-5}$	$-3.6(3)\times10^{-5}$
B_4^4	$\pm4.3(2)\times10^{-5}$	$\pm6.2(3)\times10^{-5}$

Physicists Hamiltonian:

$$\hat{H} = D'\hat{S}_z^2 + B\hat{S}_z^4 + C(\hat{S}_+^4 + \hat{S}_-^4)$$

	(cm^{-1})	(kelvin)
D'	$-0.380(2)$	$0.547(3)$
B	$-9.0(7)\times10^{-4}$	$-1.3(1)\times10^{-3}$
C	$\pm2.1(1)\times10^{-5}$	$\pm3.0(1)\times10^{-5}$

$g_{//} = 2;\ g_{\perp} = 1.94$

- D, B_4^0, $g_{//}$ from easy axis data
- B_4^4 from hard plane rotations
- $g_{\perp}$ from perpendicular data

Origin of Fast Magnetization Tunneling in Tetranuclear Nickel Single-Molecule Magnets

Synthesis of $[Ni(hmp)(MeOH)Cl]_4 \cdot H_2O$

$$NiCl_2 \cdot (H_2O)_4 + hmpH \xrightarrow{MeOH/MeONa} [Ni(hmp)(MeOH)Cl]_4$$

Polyhedron, **1999**, *18*, 909-914

hmpH =

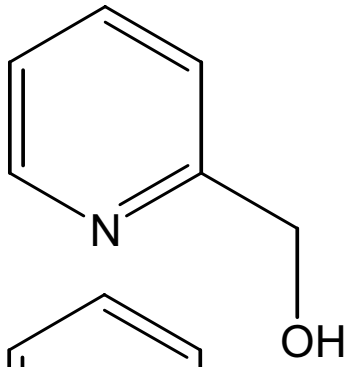

hmp^- =

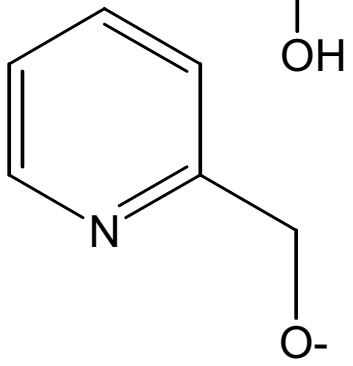

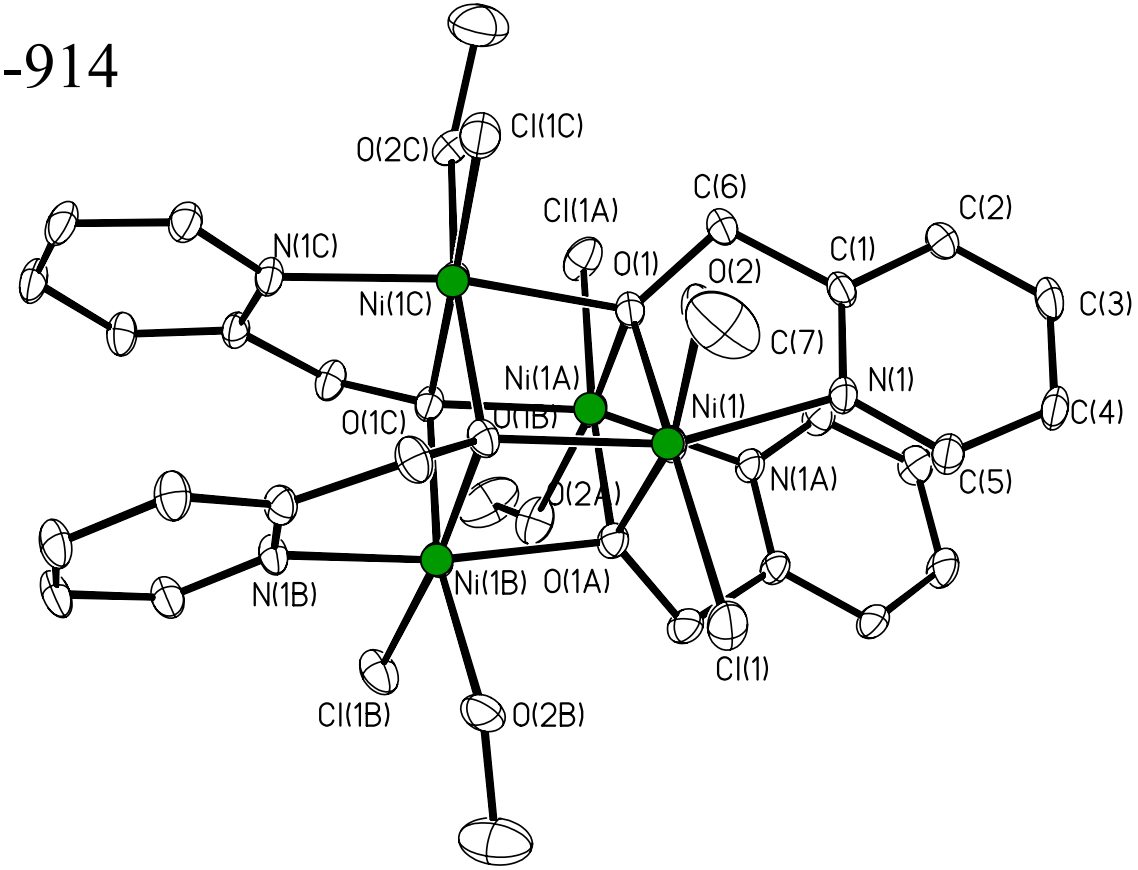

- The 4 O^s in the hmp ligands bridge 4 $S = 1$ Ni ions to form a cube
- The Ni ions couple ferromagnetically to give total spin $S = 4$
- All complexes have high (S_4) crystallographic symmetry

List of Ni_4 Cubane Samples

- $[Ni(hmp)(MeOH)Cl]_4$----------EPR, Hysteresis
- $[Ni(hmp)(EtOH)Cl]_4$ ----------EPR, Hysteresis
- $[Ni(hmp)(tBuEtOH)Cl]_4$----------**EPR**, **Hysteresis**
- $[Ni(hmp)(MeOH)Br]_4$---------- EPR, Hysteresis
- $[Ni(dbm)(MeO)(MeOH)]_4$---------- EPR, Hysteresis
- $[Ni_{0.1}Zn_{0.9}(hmp)(MeOH)Cl]_4$----------_____
- $[Ni_{0.02}Zn_{0.98}(hmp)(tBuEtOH)Cl]_4$---------- **EPR**
- $[Ni(hmp)(tBuEtOH)Br]_4$---------- EPR
- $[Ni(hmp)(CychexPrOH)Cl]_4$-------- _____, Hysteresis

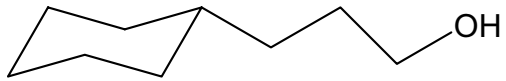

tBuEtOH =

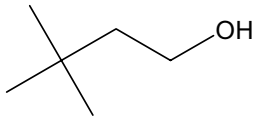

dbm =

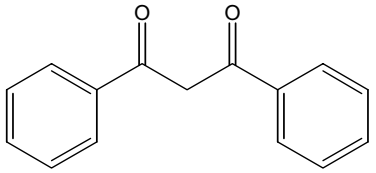

Structure of $[Ni(hmp)(t\text{-}BuEtOH)Cl]_4$

$$\hat{H} = D\hat{S}_z^{\,2} + B_4^{\,0}\hat{O}_4^{\,0} + \underline{B_4^{\,4}\hat{O}_4^{\,4}} + g\mu_B \boldsymbol{B}\cdot\hat{S}$$

hmpH =

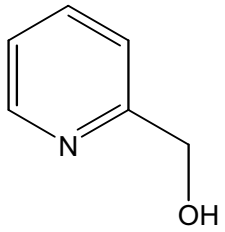

tBuEtOH =

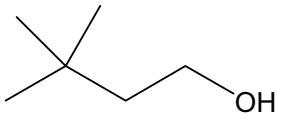

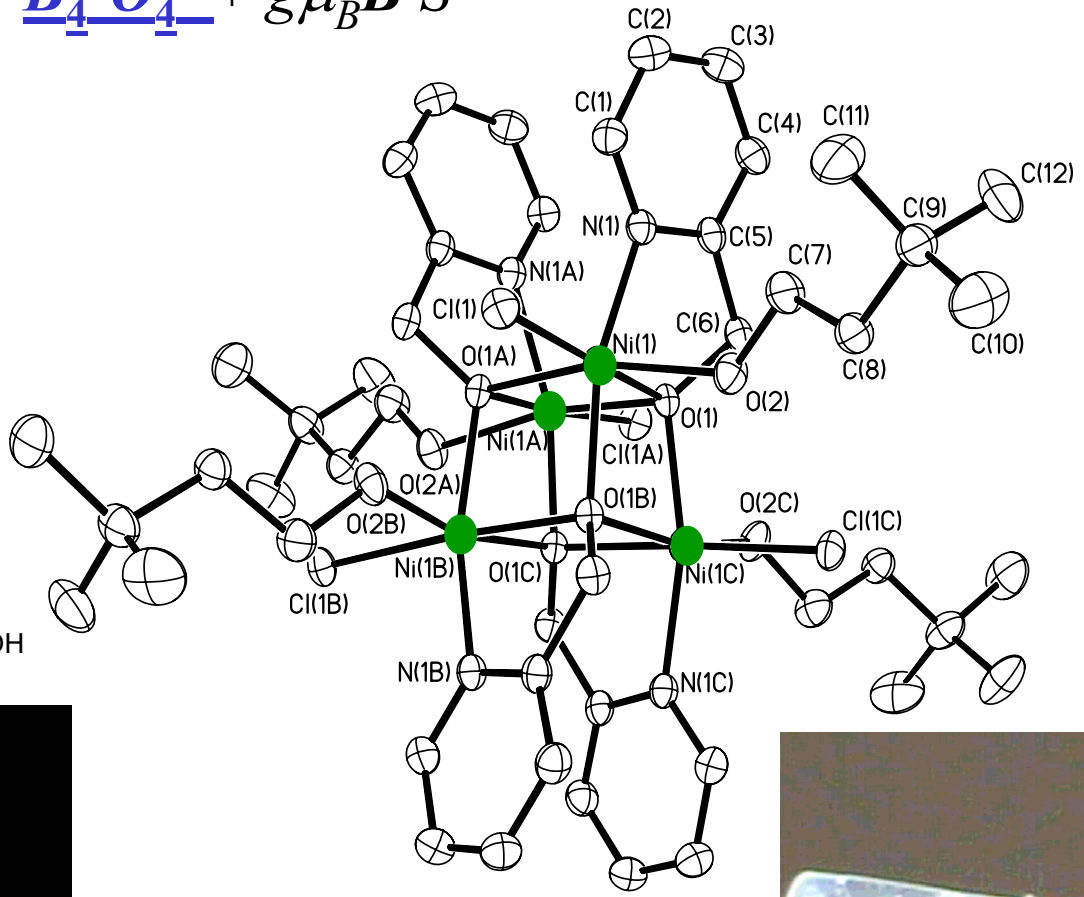

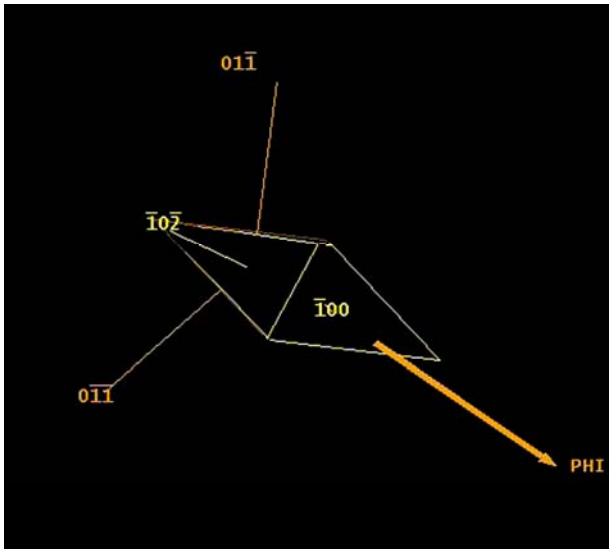

No solvent in the structure!

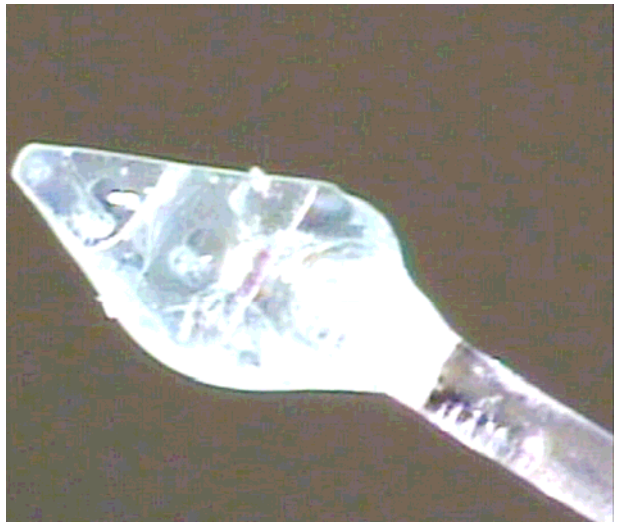

$[Ni(hmp)(t\text{-}BuEtOH)Cl]_4$ Single Crystal

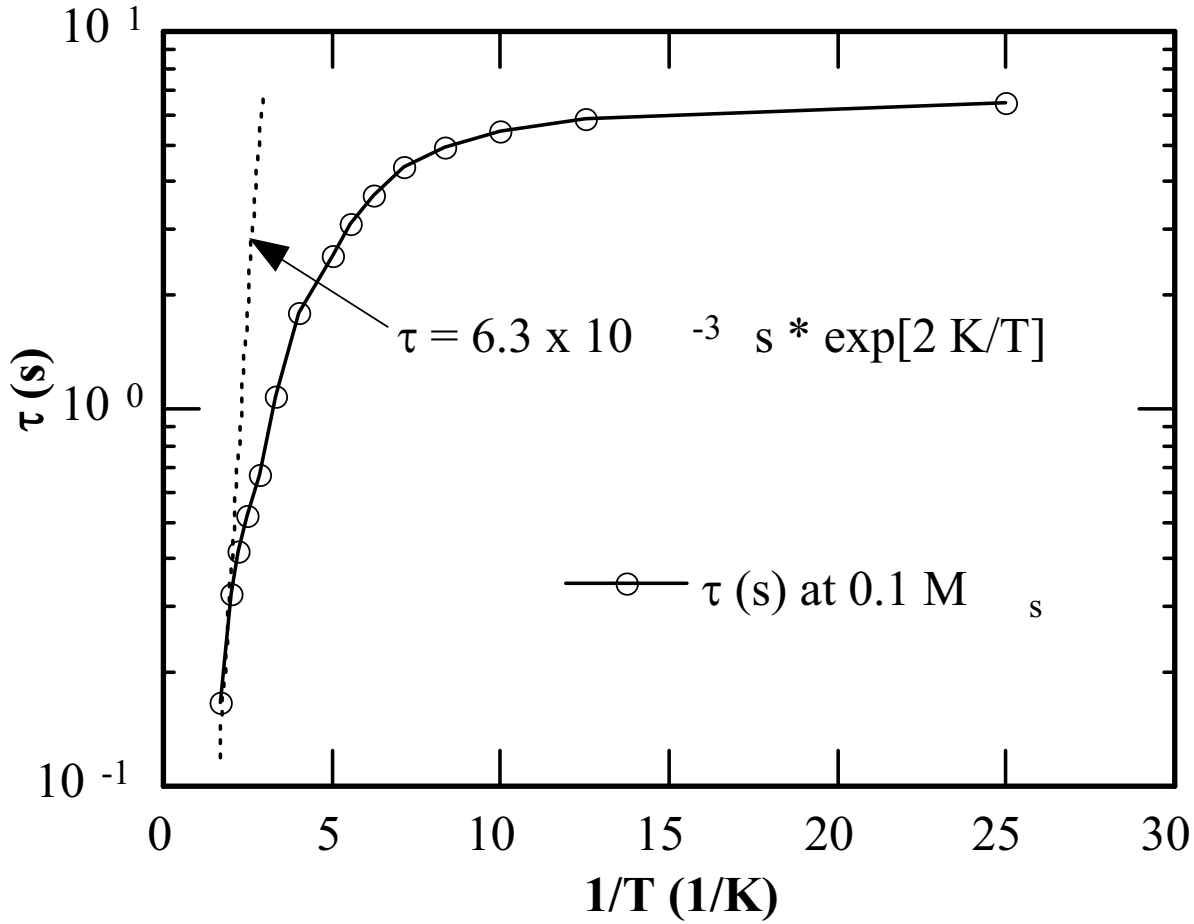

FAST!

- Temperature-independent magnetization relaxation at low temperature indicative of quantum tunneling

Single-crystal easy-axis spectra for $[Ni(hmp)(tBuEtOH)Cl]_4$

- Typical for a SMM with negative magnetocrystalline anisotropy
- Note also the splittings and additional peaks at high-T

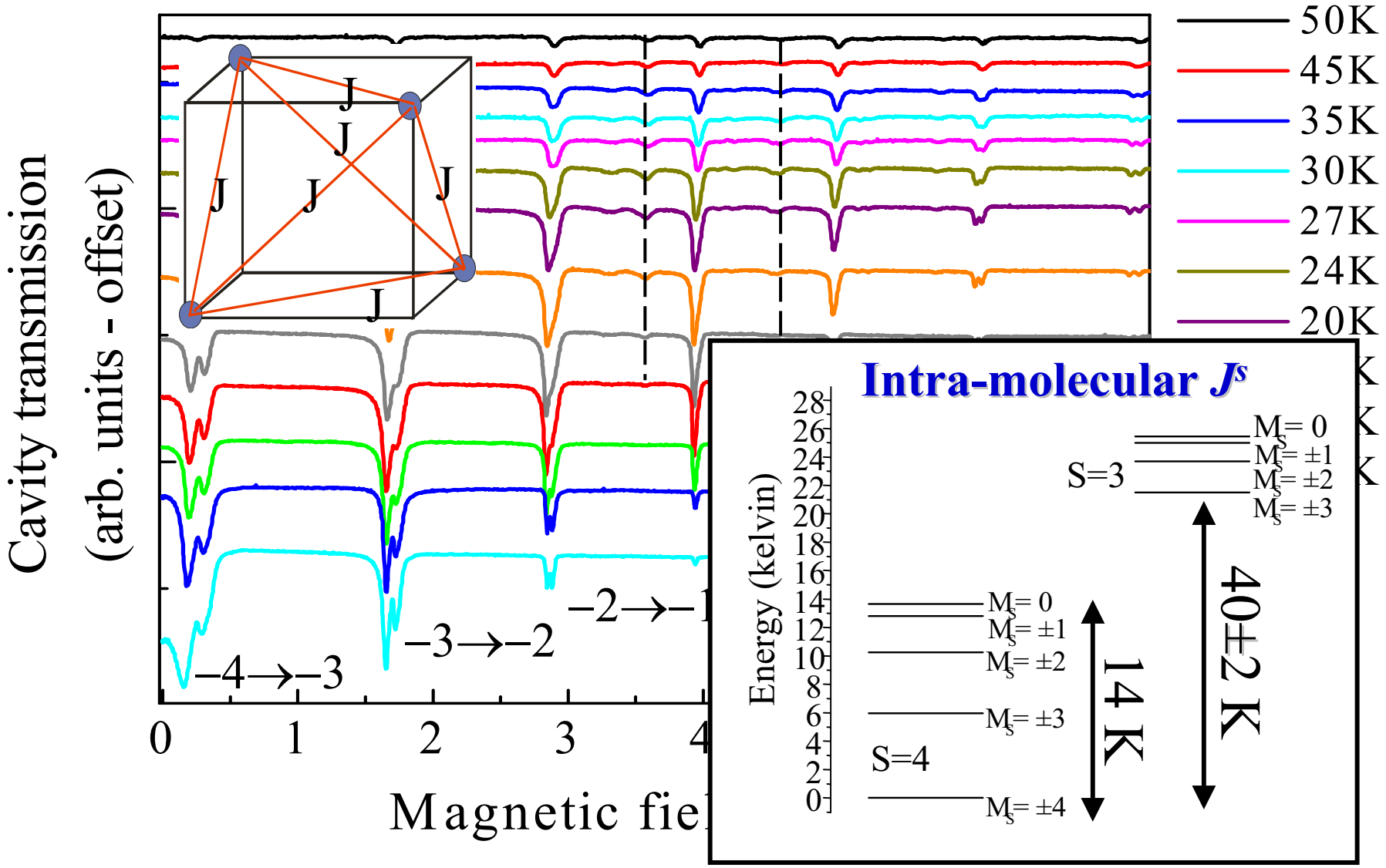

Closer look at the EPR splitting in $[Ni(hmp)(tBuEtOH)Cl]_4$

- Evidence for a structural transition at ~45 K

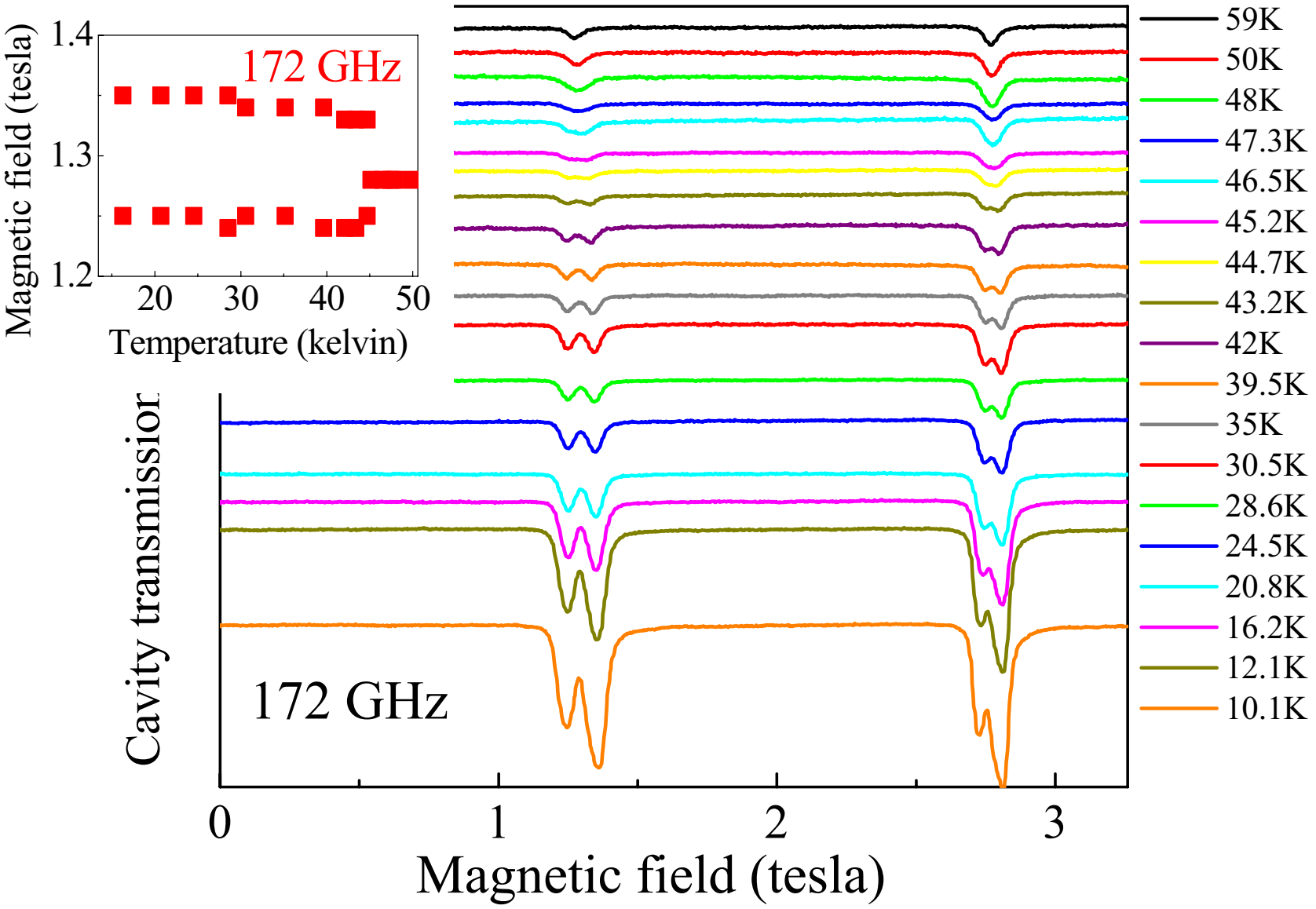

Confirmed by heat capacity and X-ray studies

- Order-disorder associated with t-Bu group

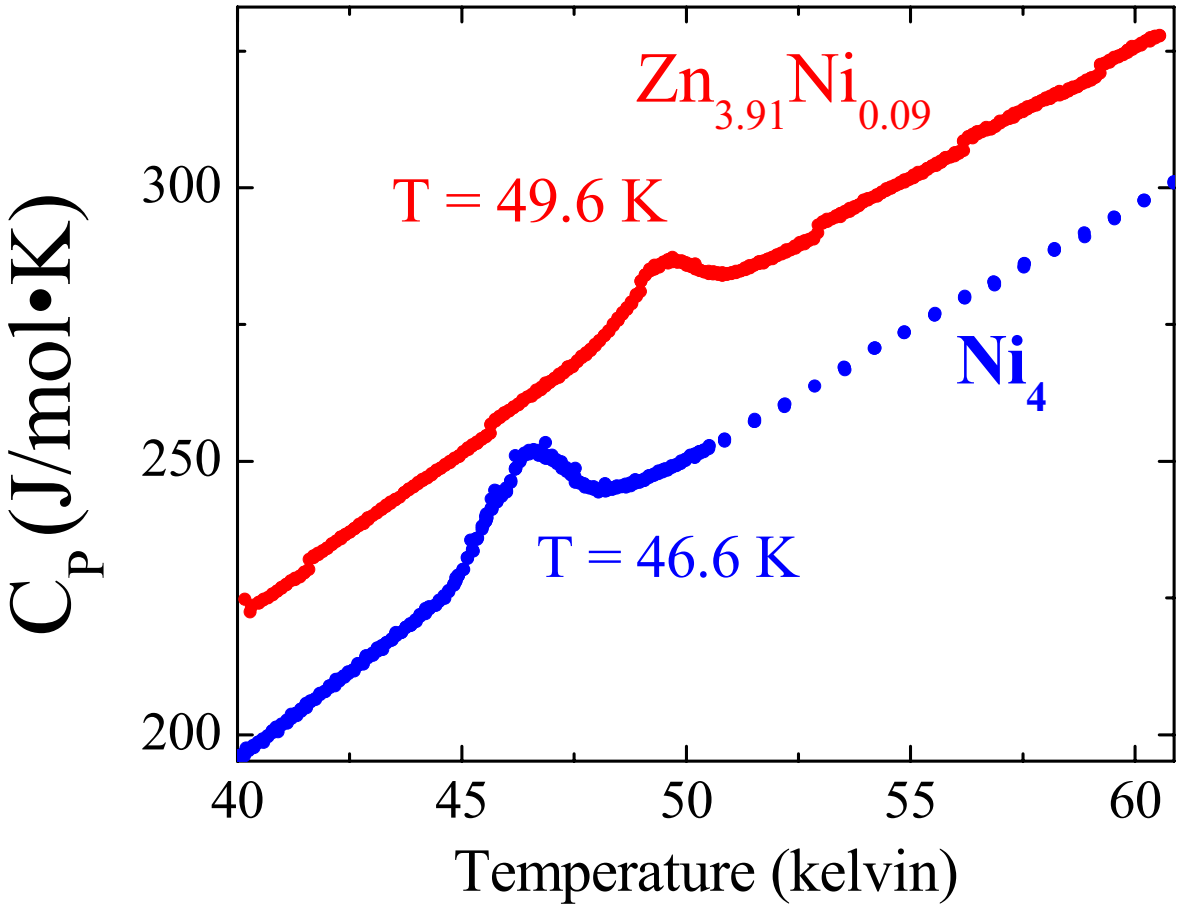

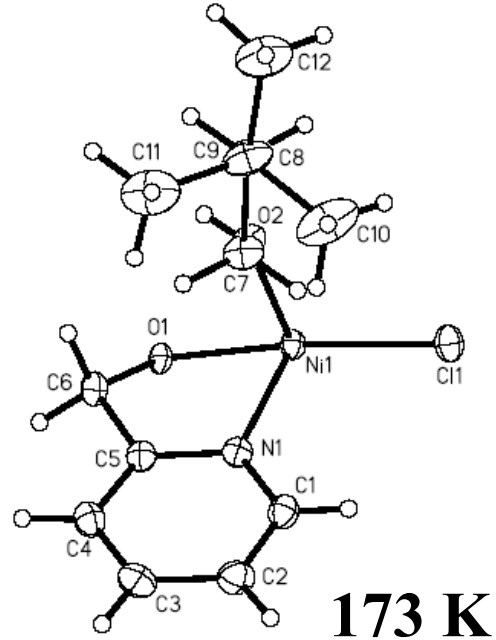

173 K

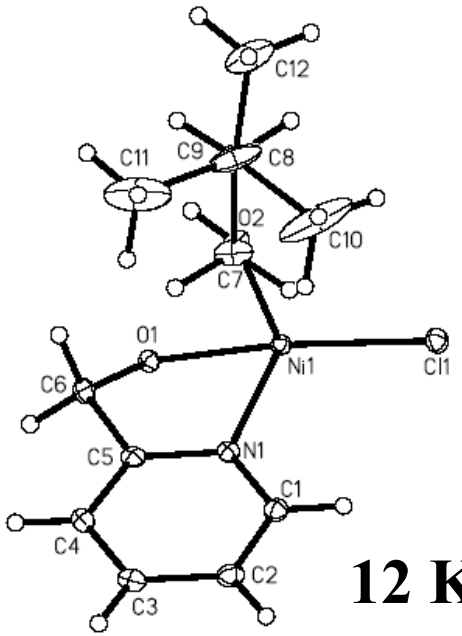

12 K

Frequency dependence of the easy axis spectra

- Enables determination of diagonal spin-Hamiltonian parameters

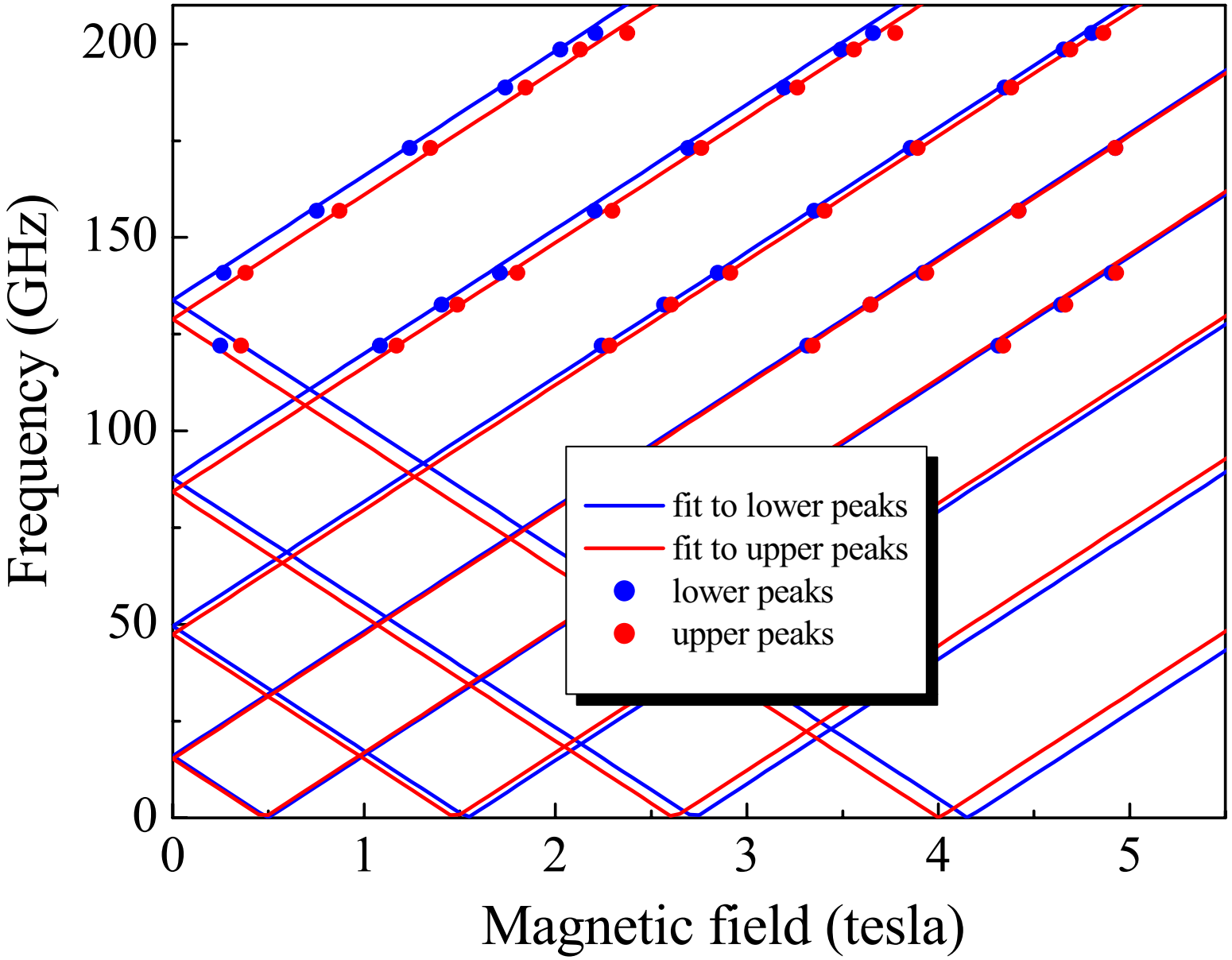

Fit to hard axis data for $[Ni(hmp)(tBuEtOH)Cl]_4$

101 GHz, hard plane rotation

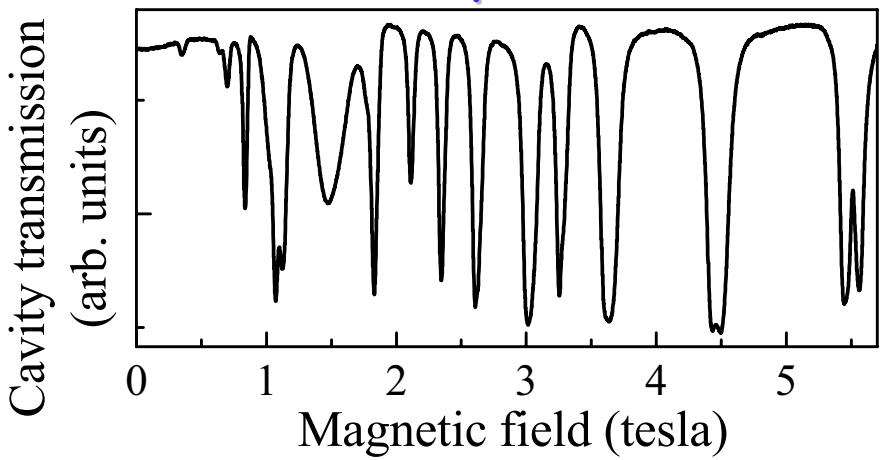

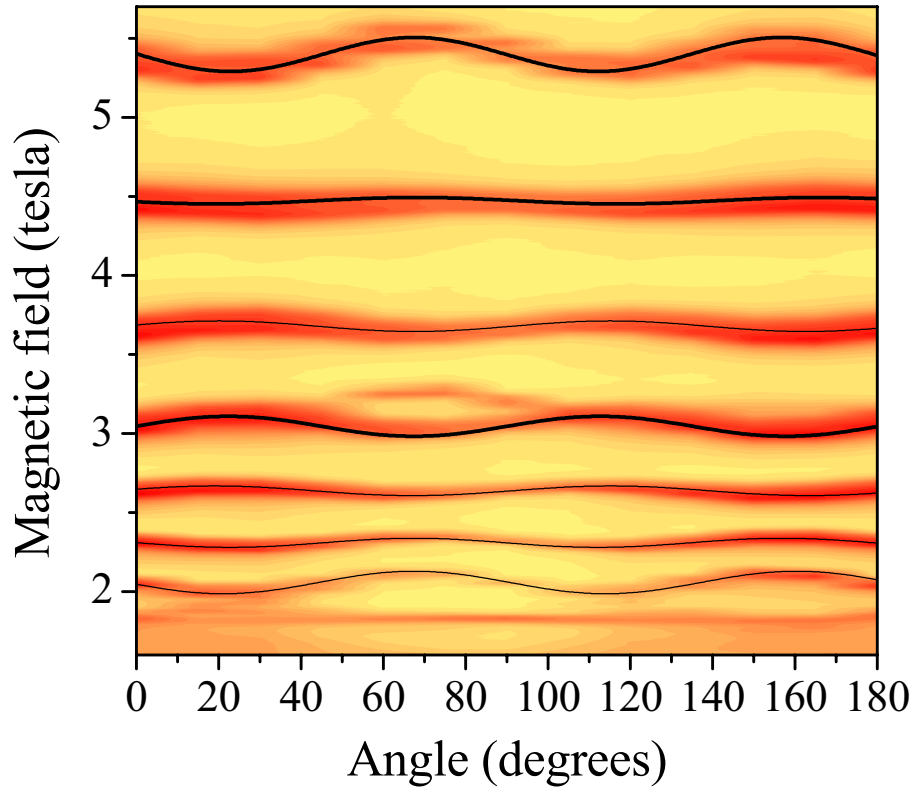

- Four-fold line shifts due to a quartic transverse interaction in $\mathcal{H}_T$
- B_4^4 is the only free parameter in the fit

S. Hill et al., PRL **90,** 217204 (2003)

$$\frac{1}{2} B_4^4 \left(\hat{S}_+^4 + \hat{S}_-^4 \right)$$

$$B_4^4 = 4 \times 10^{-4}\ \mathrm{cm}^{-1}$$

- Very effective at mixing $M_s = \pm 4$ ground states.
- 2nd order perturbation.
- 12 MHz tunnel splitting!

Spin-Hamiltonian parameters for $[Ni(hmp)(ROH)Cl]_4$

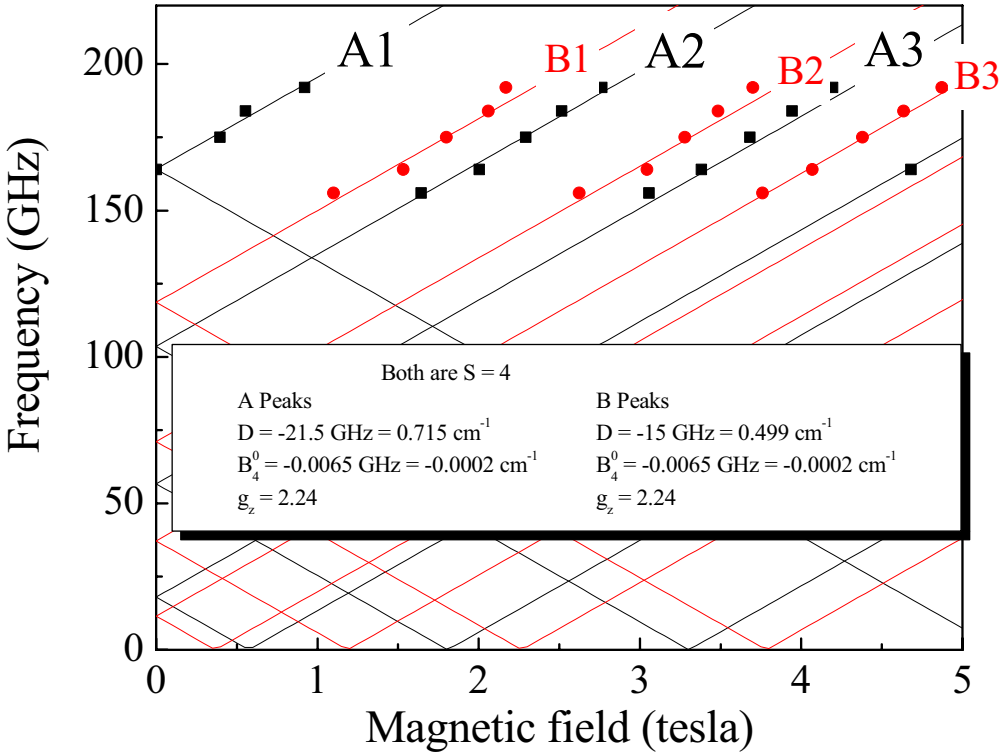

- The ability to deconvolute all of the various contributions to these spectra would not have been possible via powder EPR
- Also, the broad lines observed for the strongly exchanging complexes are best observed via direct absorption measurements

J. Appl. Phys. 93, 7807 (2003)

		D (cm^{-1})	B_4^0 (cm^{-1})	g_z	B_4^4 (cm^{-1})
$[Ni(t\text{-}BuEtOH)Cl]_4$	lower peaks	-0.600	-0.00012	2.3	± 0.0004
	upper peaks	-0.577	-0.00012	2.3	± 0.0004
$[Ni(EtOH)Cl]_4$	lower peaks	-0.673	-0.00012	2.2	
	upper peaks	-0.609	-0.00012	2.2	
$[Ni(MeOH)Cl]_4$	lower peaks	-0.715	-0.0002	2.2	
	upper peaks	-0.499	-0.0002	2.2	

Evaluation of the Ni^{II} single-ion spin Hamiltonian

$S = 1$

$[Ni_{0.02}Zn_{0.98}(hmp)(tBuEtOH)Cl]_4$

$NiZn_3$

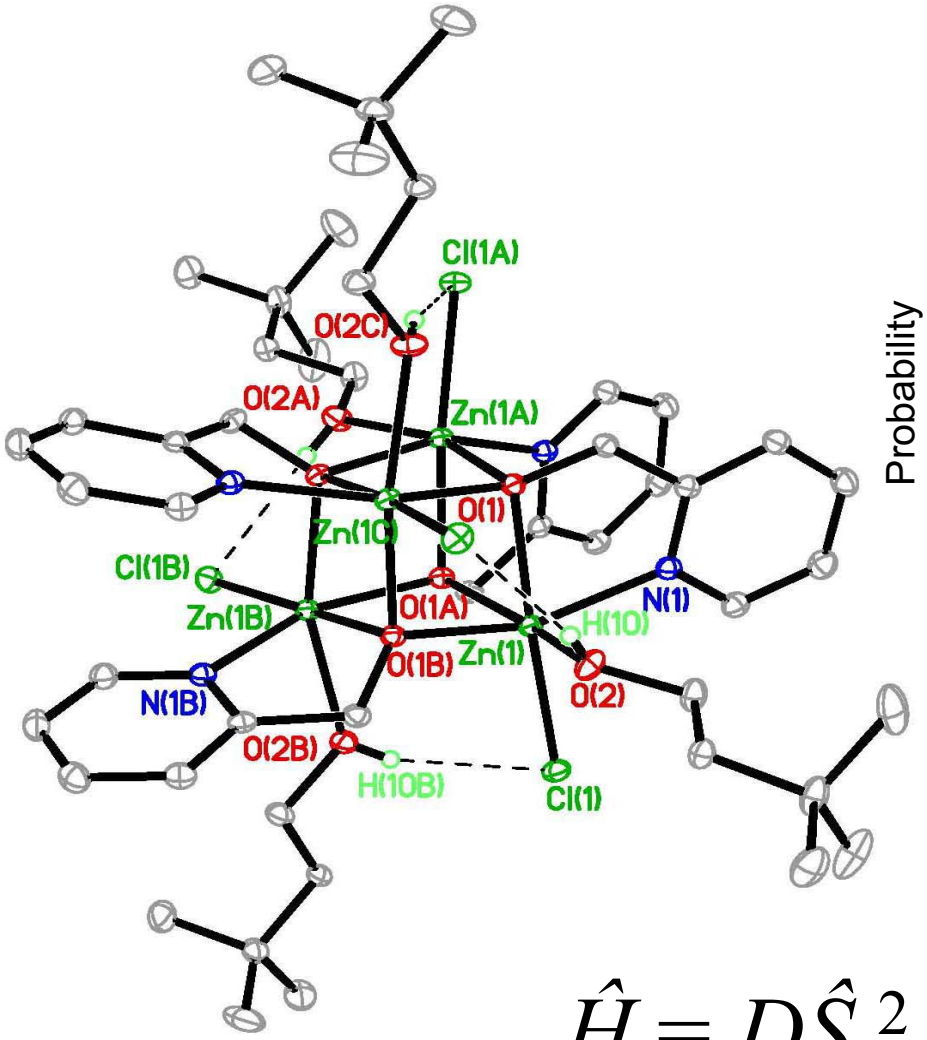

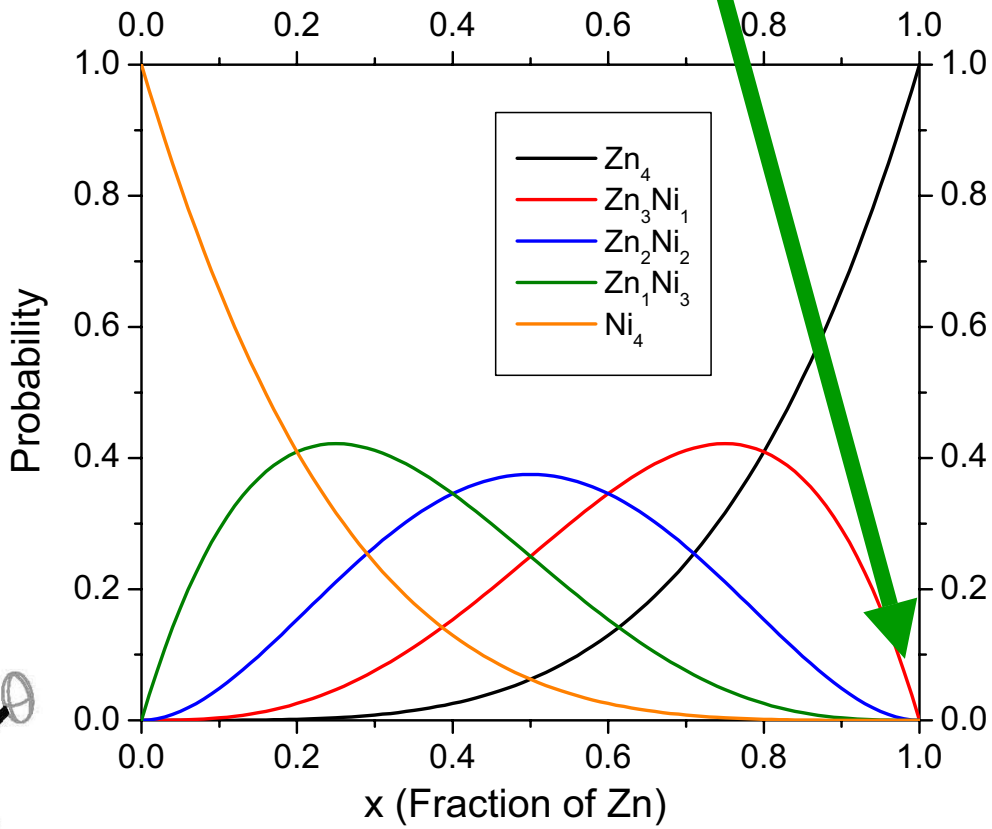

$$\hat{H} = D\hat{S}_z^2 + E(\hat{S}_x^2 - \hat{S}_y^2) + g\mu_B \boldsymbol{B}\cdot\hat{S}$$

Frequency-dependence

- Single-ion tensors are not collinear ⇒ multiple EPR fine structures

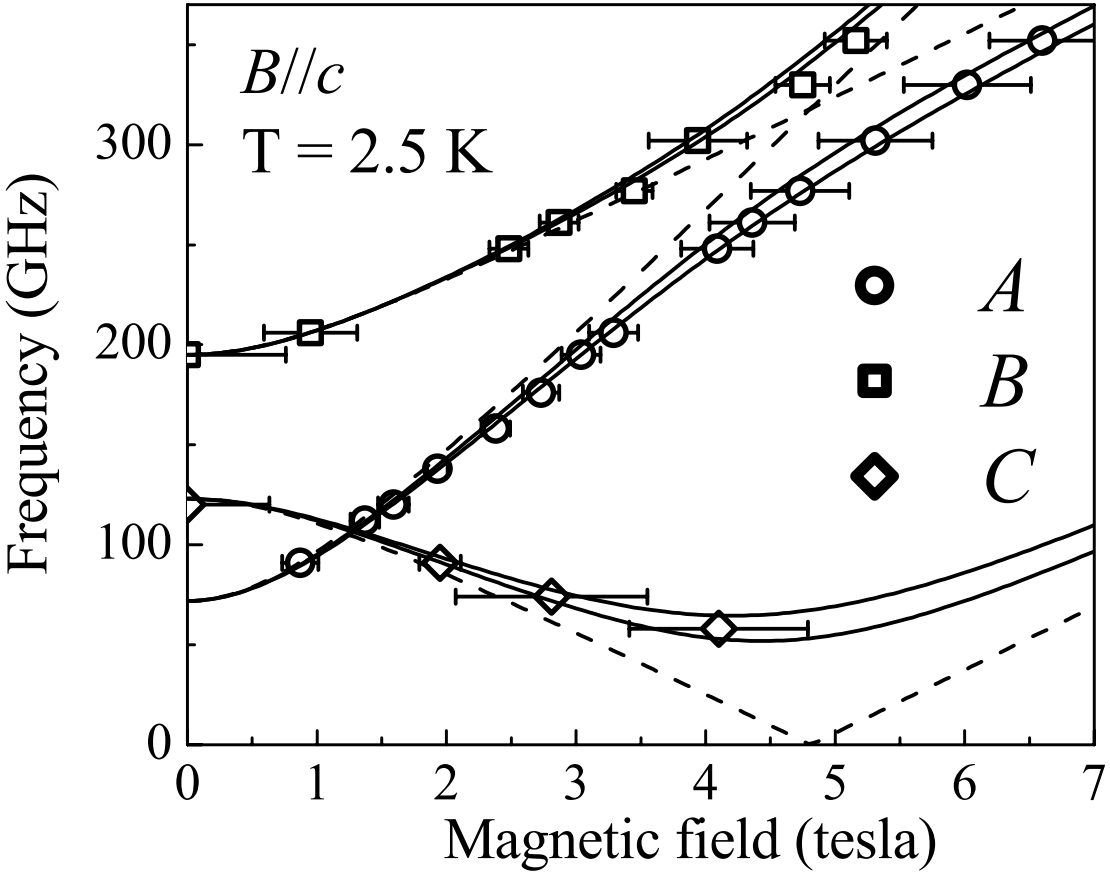

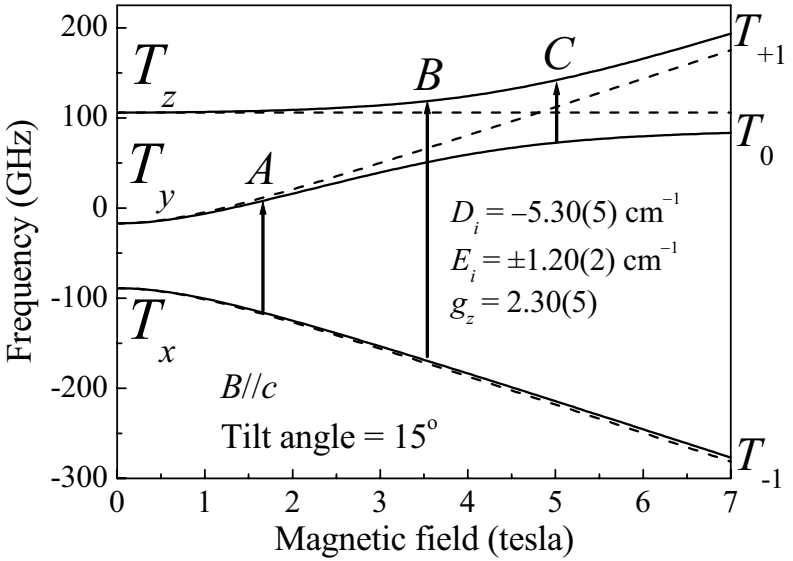

Initialize *D* and *E* parameters from Frequency dep. ⇒

D = –5.30(5) cm^{-1}
E = ±1.20(1) cm^{-1}
$g_{//}$ = 2.30(5)
tilt = 15°

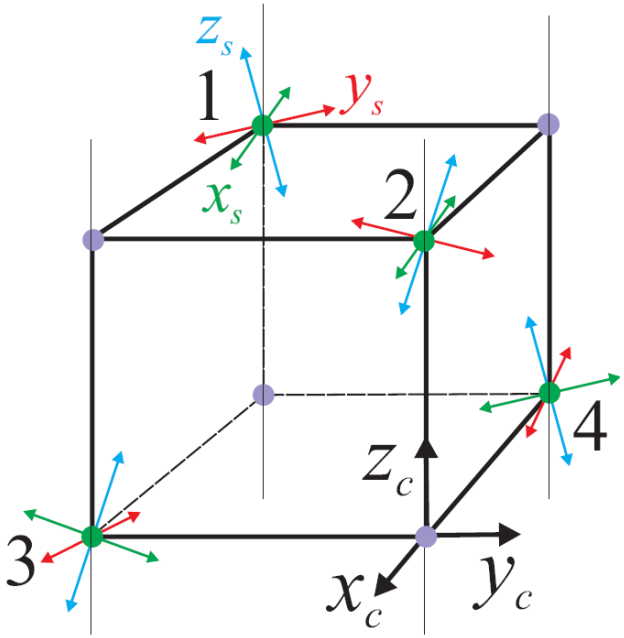

Angle-dependence to find orientation of zfs interaction

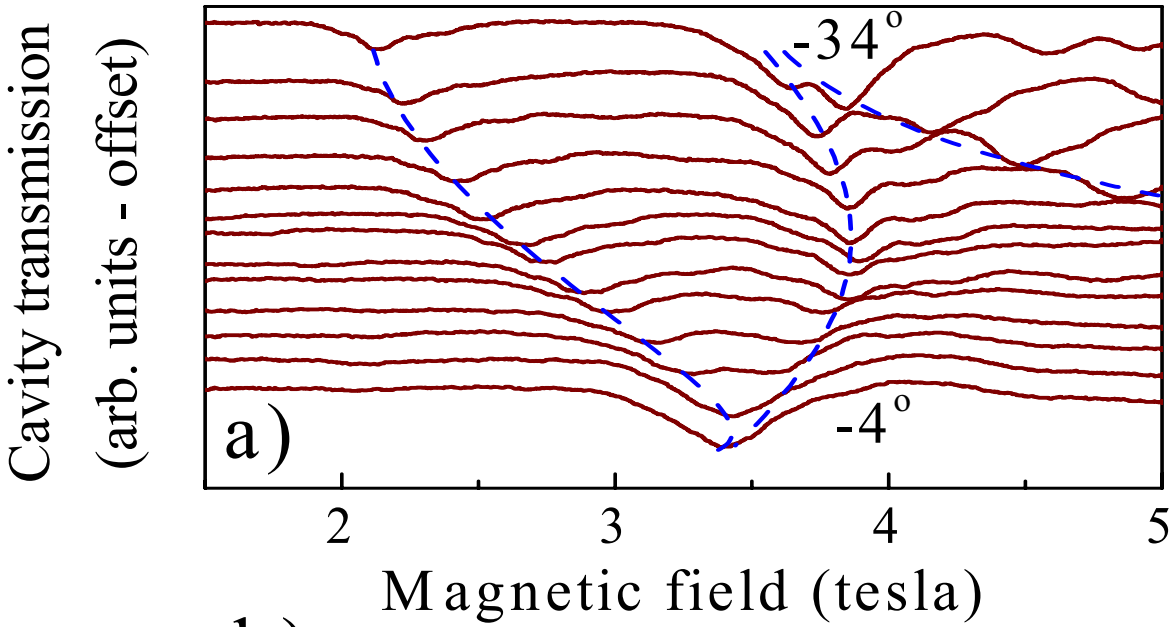

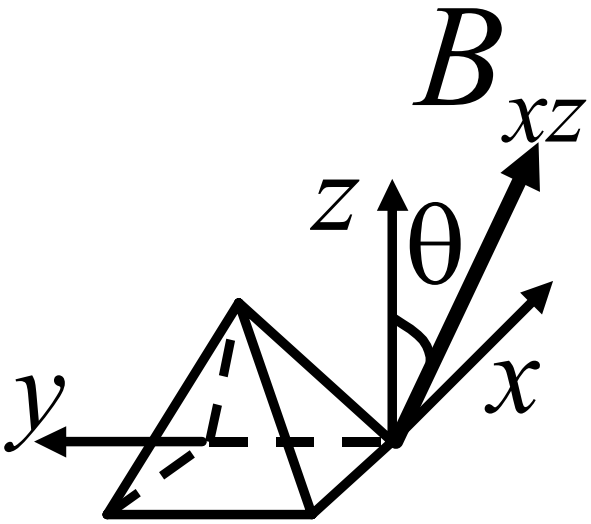

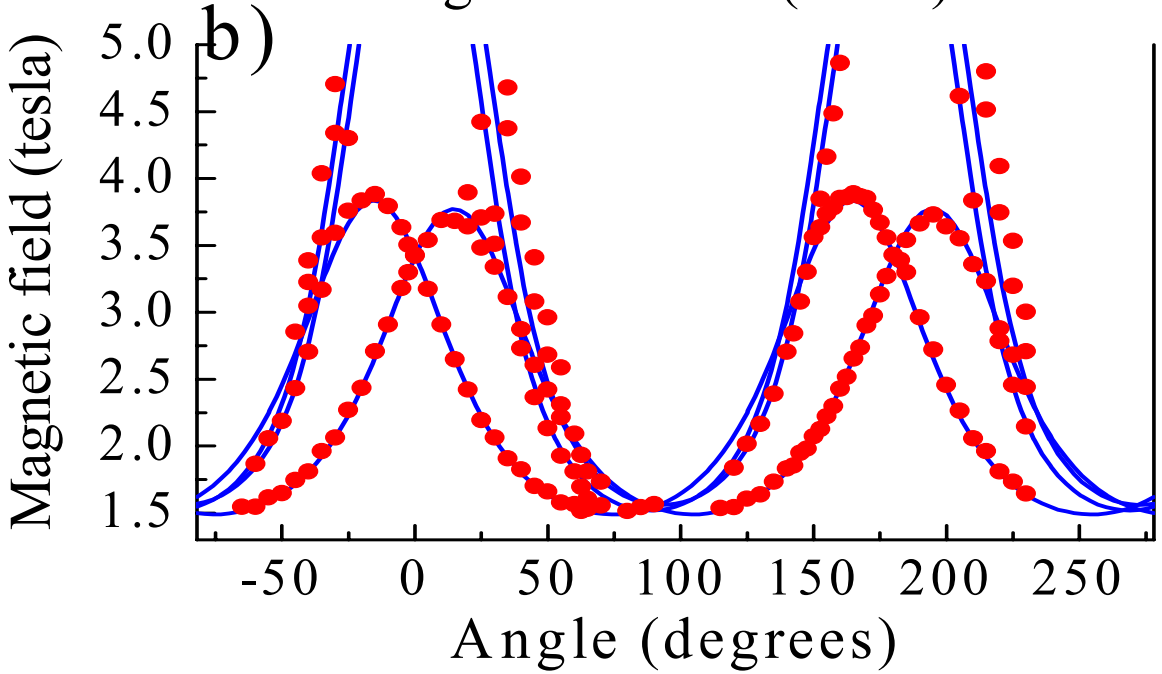

3 planes of rotation. One single fit to all of the data.

Angle-dependence to find orientation of zfs interaction

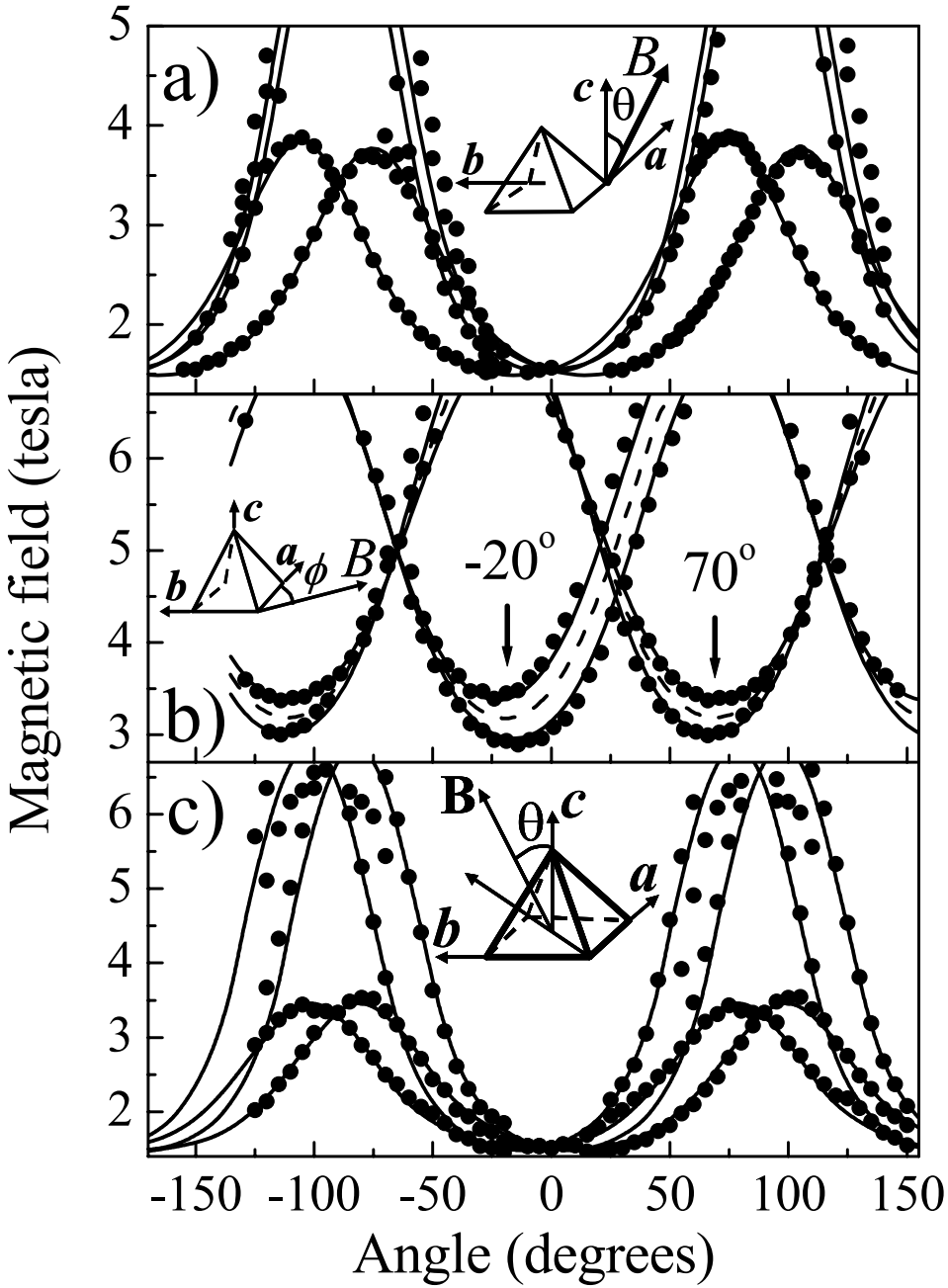

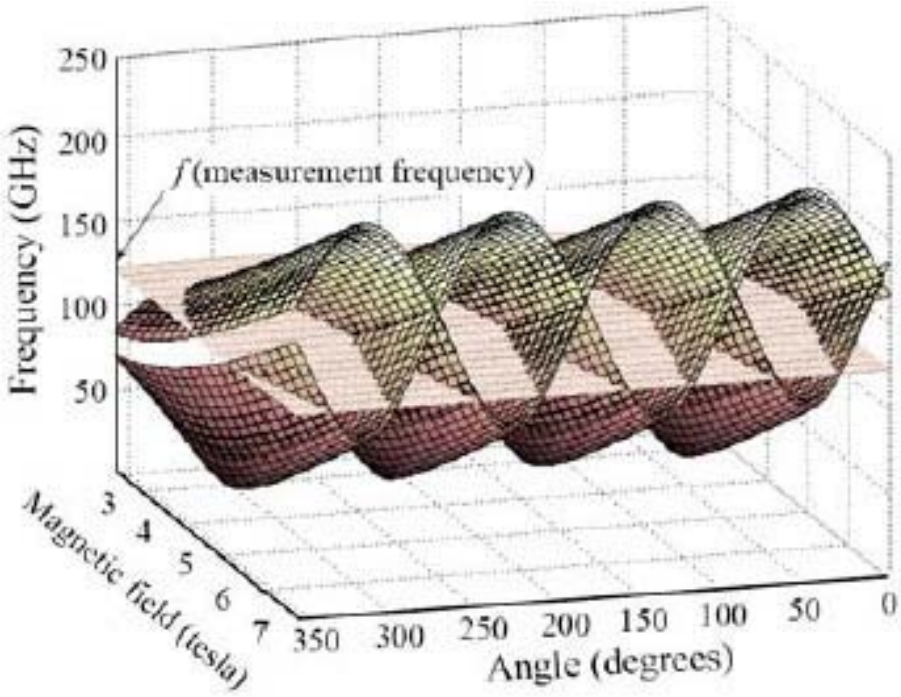

E.-C. Yang et al., published in Inorg. Chem.(last week)

Relation between Ni^{II} and Ni_4 spin parameters

$$\overline{\overline{D}}_{local} = \begin{bmatrix} -D/3+E & 0 & 0 \\ 0 & -D/3-E & 0 \\ 0 & 0 & 2D/3 \end{bmatrix}$$

$$\overline{\overline{D}}_{crystal} = \overline{\overline{A}}^{-1}\,\overline{\overline{D}}_{local}\,\overline{\overline{A}}$$

$\overline{\overline{A}}$ is Euler matrix

$$\boxed{\overline{\overline{D}}_{total} = d_1\overline{\overline{D}}_1 + d_2\overline{\overline{D}}_2 + d_3\overline{\overline{D}}_3 + d_4\overline{\overline{D}}_4 + d_{12}\overline{\overline{D}}_{12} + d_{13}\overline{\overline{D}}_{13} + d_{14}\overline{\overline{D}}_{14} + d_{23}\overline{\overline{D}}_{23} + d_{24}\overline{\overline{D}}_{24} + d_{34}\overline{\overline{D}}_{34}}$$

$D_i \equiv$ single-ion zfs tensors (5 cm^{-1}); $D_{ij} \equiv$ dipolar couplings (0.1 cm^{-1})

$$\boxed{\overline{\overline{D}}_{total} = \tfrac{1}{28}\overline{\overline{D}}_1 + \tfrac{1}{28}\overline{\overline{D}}_2 + \tfrac{1}{28}\overline{\overline{D}}_3 + \tfrac{1}{28}\overline{\overline{D}}_4 + \tfrac{2}{28}\overline{\overline{D}}_{12} + \tfrac{2}{28}\overline{\overline{D}}_{13} + \tfrac{2}{28}\overline{\overline{D}}_{14} + \tfrac{2}{28}\overline{\overline{D}}_{23} + \tfrac{2}{28}\overline{\overline{D}}_{24} + \tfrac{2}{28}\overline{\overline{D}}_{34}}$$

$$\boxed{\overline{\overline{D}}_{total} \approx \tfrac{1}{28}\overline{\overline{D}}_1 + \tfrac{1}{28}\overline{\overline{D}}_2 + \tfrac{1}{28}\overline{\overline{D}}_3 + \tfrac{1}{28}\overline{\overline{D}}_4}$$

$$\overline{\overline{D}}_{total} = \begin{bmatrix} 0.229 & 0 & 0 \\ 0 & 0.229 & 0 \\ 0 & 0 & -0.459 \end{bmatrix} cm^{-1}$$

Traceless, i.e. $E = 0$

$D_{total} = -0.69\ cm^{-1}$

$D_{actual} = -0.60\ cm^{-1}$

Need to relate the Ni^{II} Hamiltonian to the 4th order Ni_4 Hamiltonian

Quantum entanglement in $[Mn_4]_2$ dimers

Antiferromagnetic exchange in a dimer of Mn_4 SMMs

$[Mn_4O_3Cl_4(O_2CEt)_3(py)_3]$

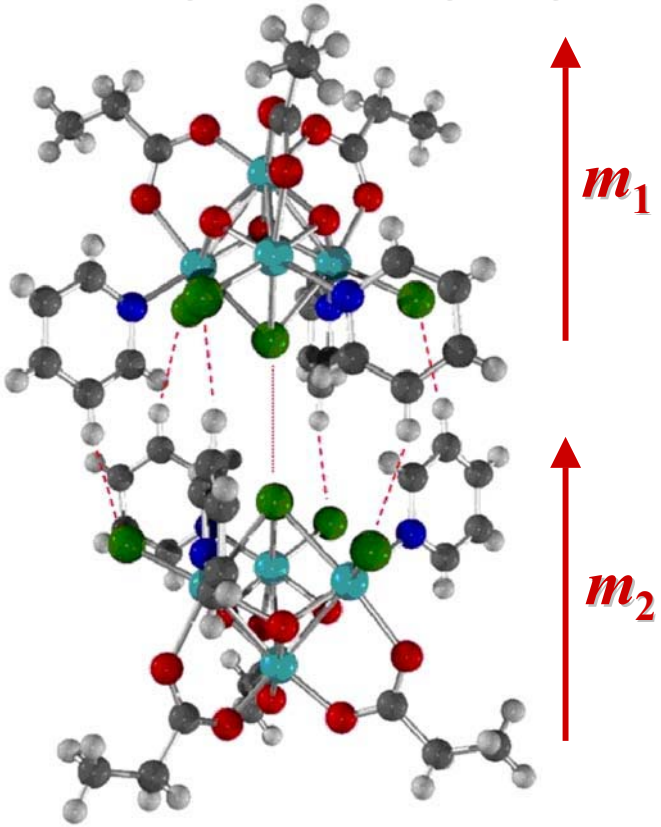

Monomer Zeeman diagram

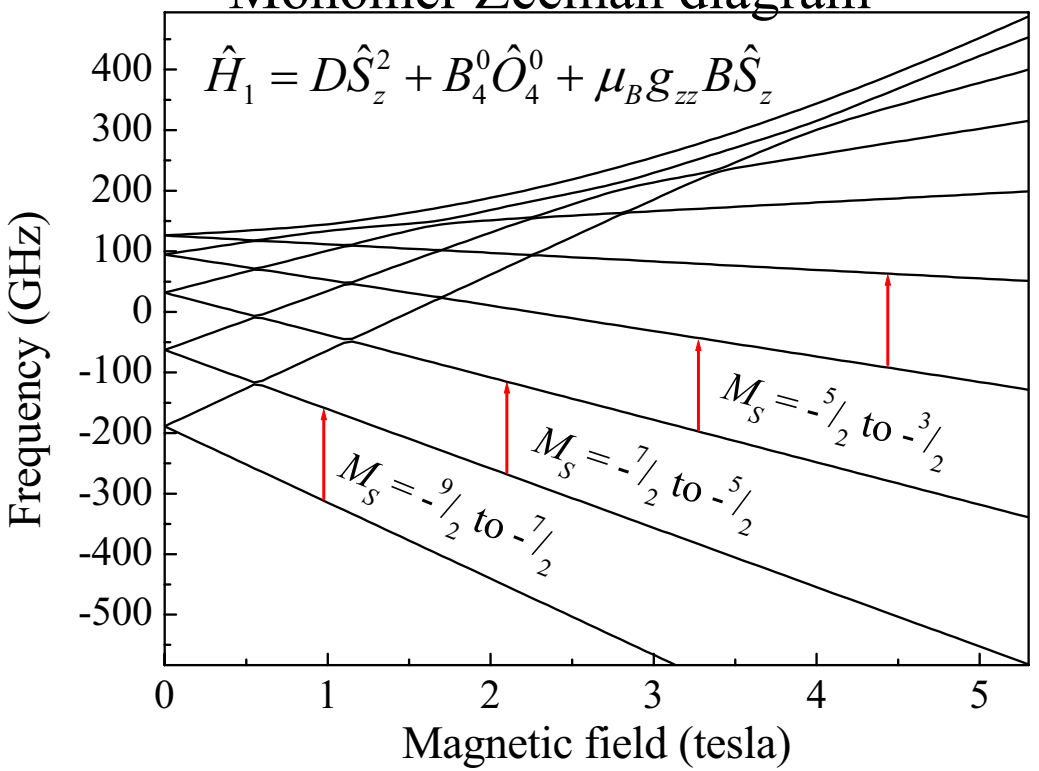

$D = -0.75(1)$ K

$B_0^4 = 5 \times 10^{-5}$ K

$J \approx 0.12(1)$ K

HFEPR for high symmetry (C_{3v}) Mn_4 **monomer**

$[Mn_4O_3(OSiMe_3)(O_2CEt)_3(dbm)_3]$

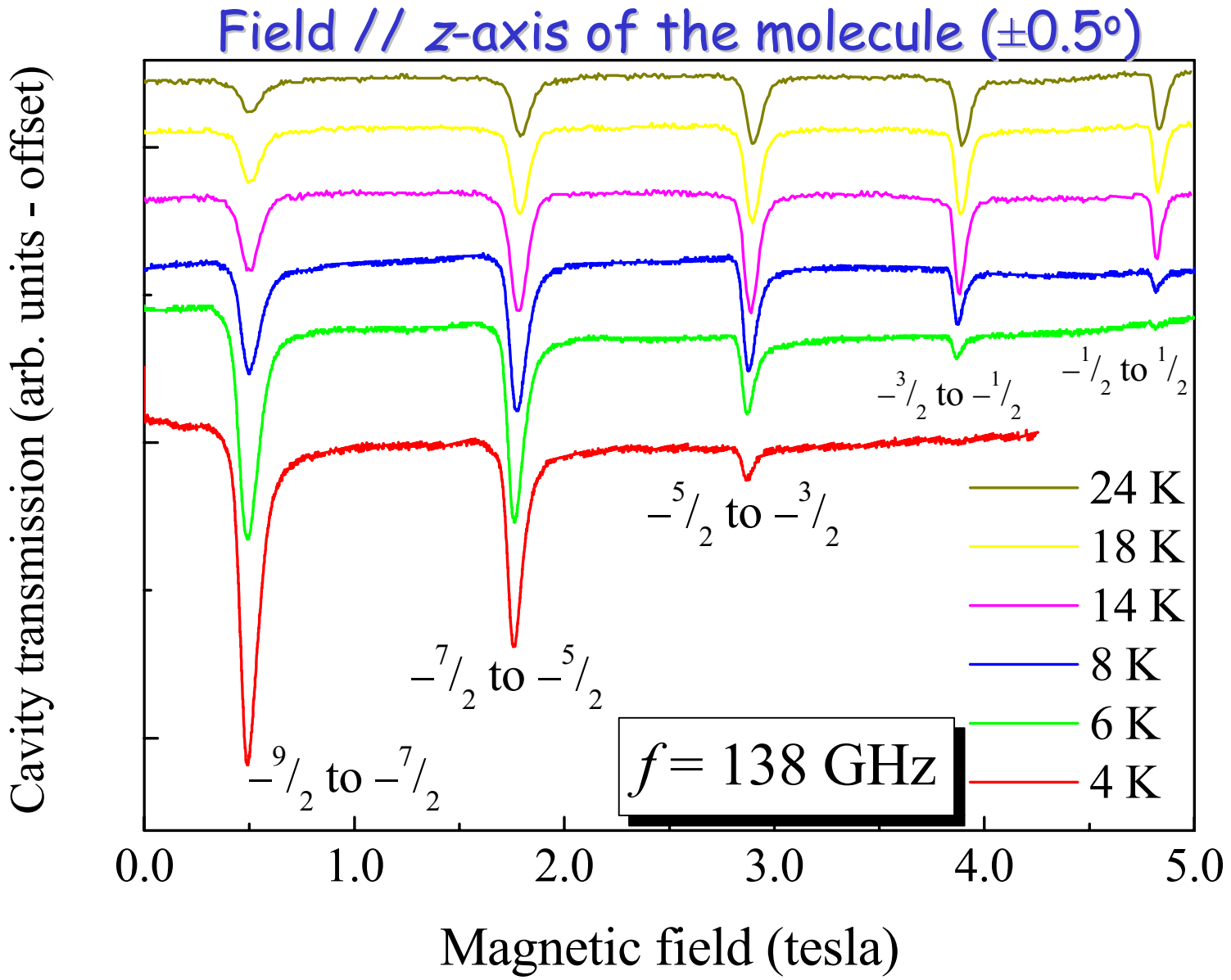

Antiferromagnetic exchange in a dimer of Mn_4 SMMs

$[Mn_4O_3Cl_4(O_2CEt)_3(py)_3]$

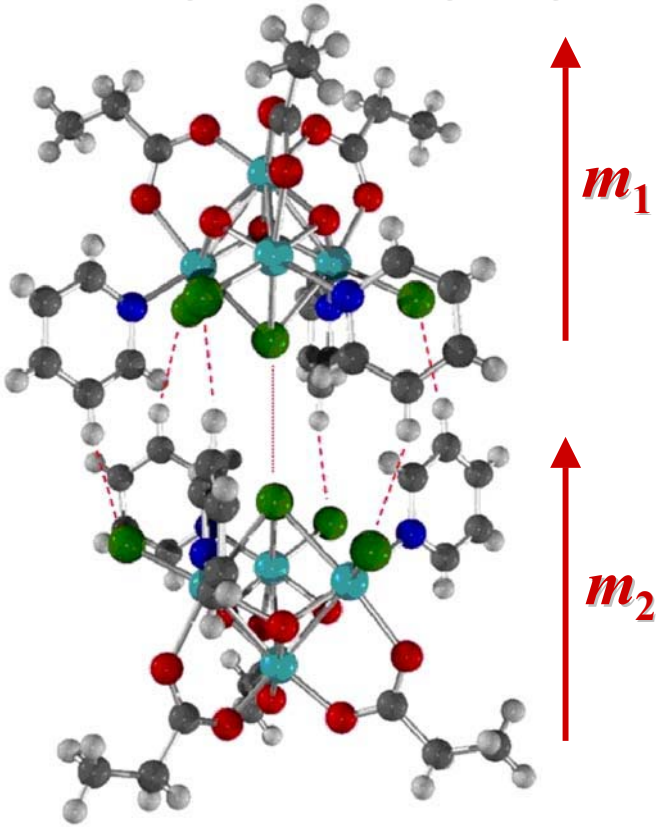

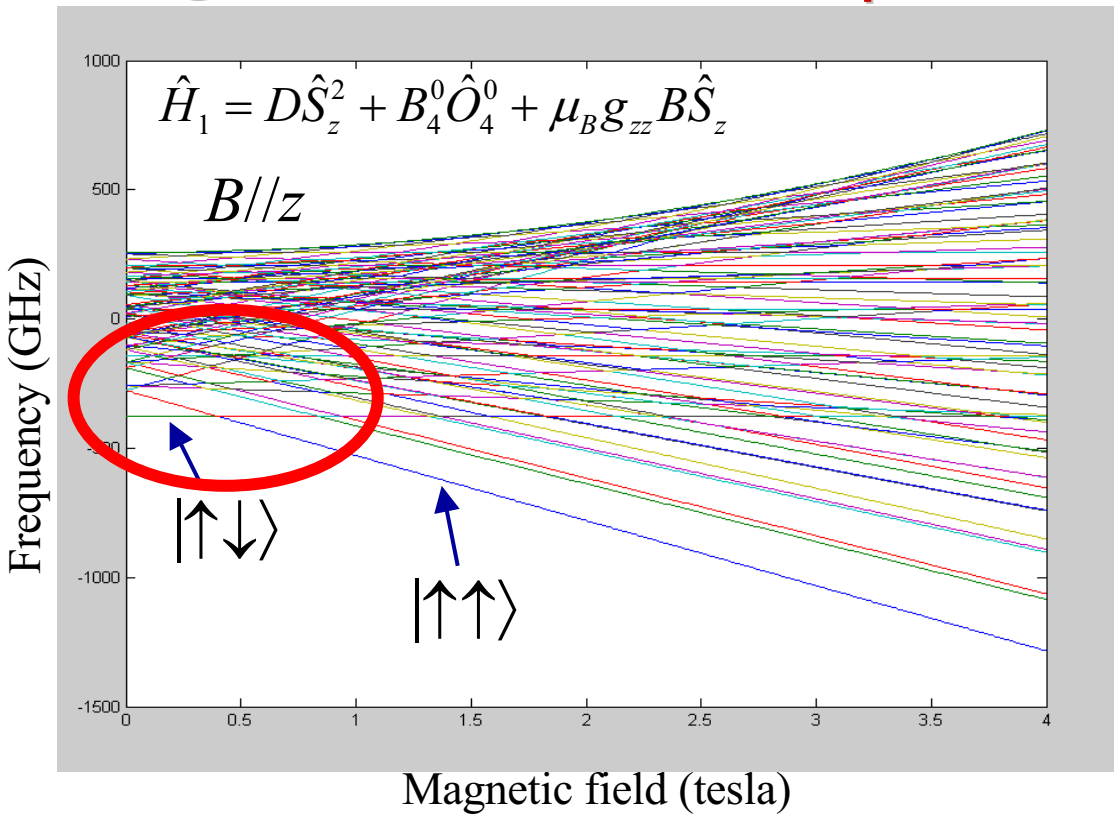

$D = -0.75(1)$ K

$B_0^4 = 5 \times 10^{-5}$ K

$J \approx 0.12(1)$ K

$$\hat{H} = \hat{H}_1 + \hat{H}_2 + J\hat{S}_1 \cdot \hat{S}_2$$

Multiplicity increases from $(2S+1)$ to $(2S+1)^2$

Antiferromagnetic exchange in a dimer of Mn_4 SMMs

$[Mn_4O_3Cl_4(O_2CEt)_3(py)_3]$

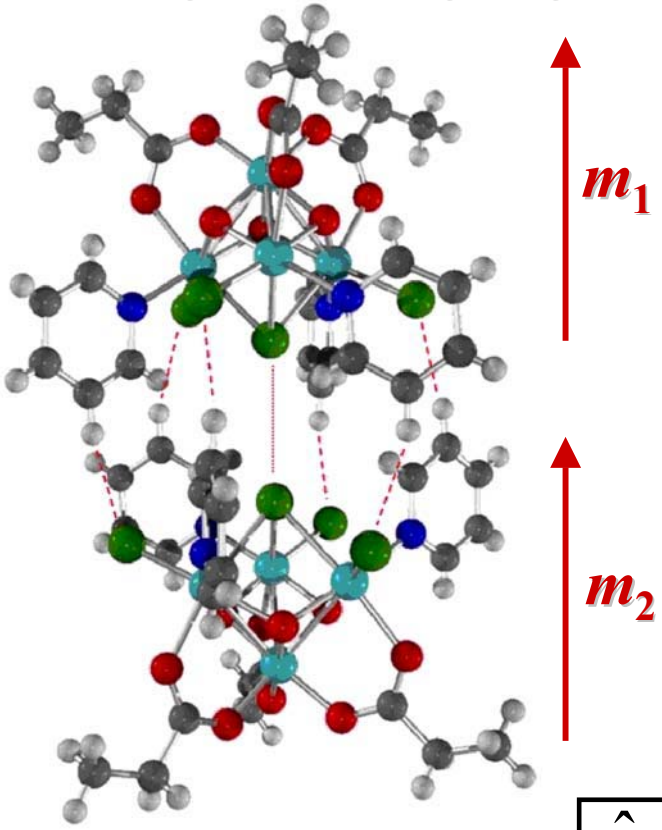

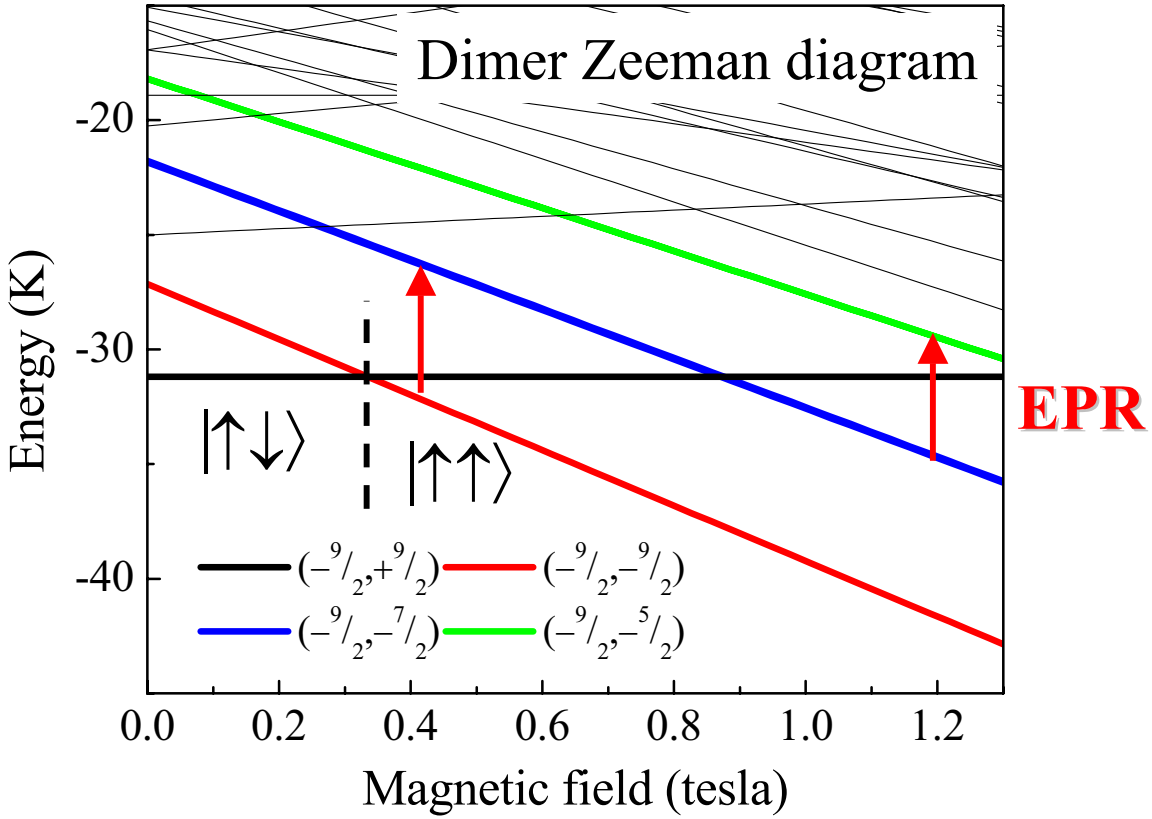

$D = -0.75(1)$ K

$B_0^4 = 5 \times 10^{-5}$ K

$J \approx 0.12(1)$ K

$$\hat{H} = \hat{H}_1 + \hat{H}_2 + J\hat{S}_1 \cdot \hat{S}_2 \approx \hat{H}_1 + \hat{H}_2 + J\hat{S}_{z1}\hat{S}_{z2}$$

$$E \approx D\left(m_1^2 + m_2^2\right) + g\mu_B B\left(m_1 + m_2\right) + Jm_1m_2$$

- Bias should shift the single spin (monomer) EPR transitions.

Wolfgang Wernsdorfer, George Christou, et al., *Nature*, **2002**, 406-409

Systematic control of coupling between SMMs - Entanglement

This scheme in the same spirit as proposals for multi-qubit devices based on quantum dots

D. Loss and D.P. DiVincenzo, Phys. Rev. A **57**, 120 (1998).

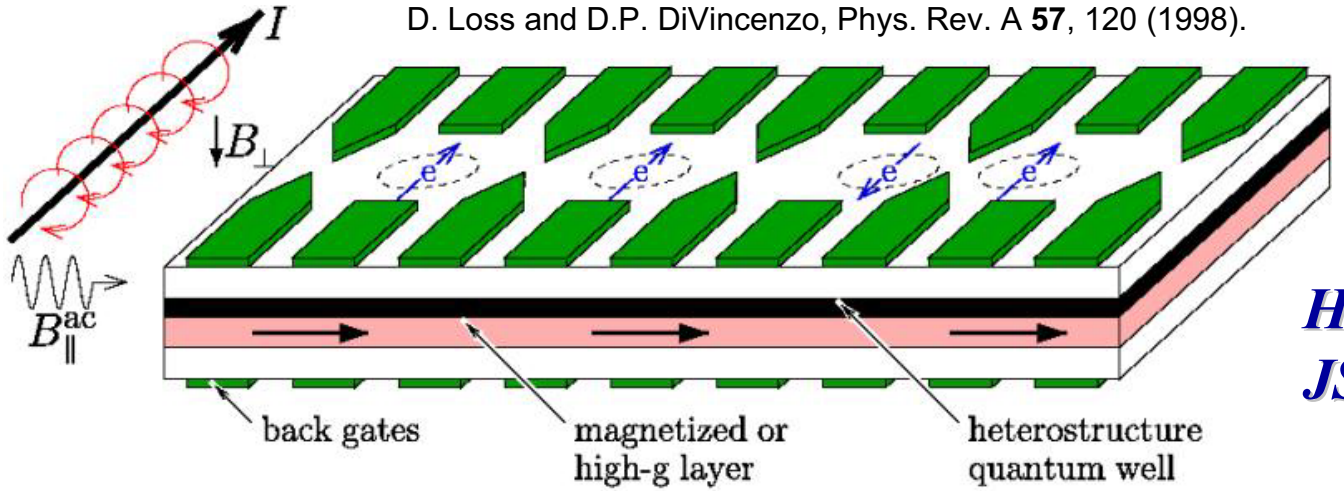

Heisenberg: $J\hat{S}_1.\hat{S}_2$

- Quantum mechanical coupling caused by the transverse (off-diagonal) parts of the exchange interaction $J_{xy}(\hat{S}_{x1}\hat{S}_{x2} + \hat{S}_{y1}\hat{S}_{y2})$.
- This term causes the entanglement, *i.e.* **it truly mixes** $|m_{z1},m_{z2}\rangle$ **basis states**, resulting in co-tunneling and EPR transitions involving **two-spin rotations**.
- CAN WE OBSERVE THIS?

$S_1 = S_2 = {}^9/_2$; multiplicity of levels = $(2S_1 + 1)(2S_2 + 1) = 100$

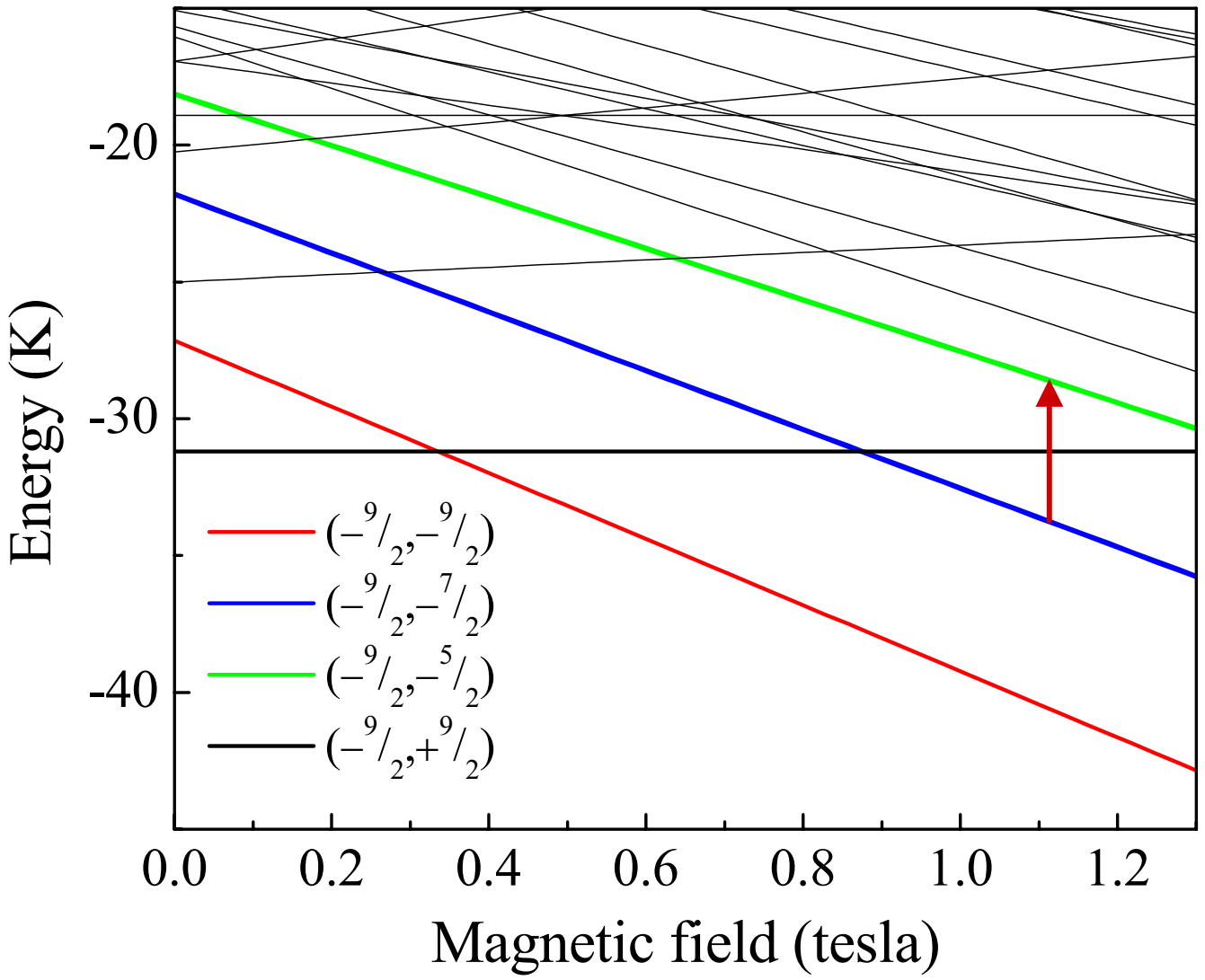

Look for additional splitting (multiplicity) and symmetry effects (selection rules) in EPR.

$S_1 = S_2 = {}^9/_2$; multiplicity of levels = $(2S_1 + 1)(2S_2 + 1) = 100$

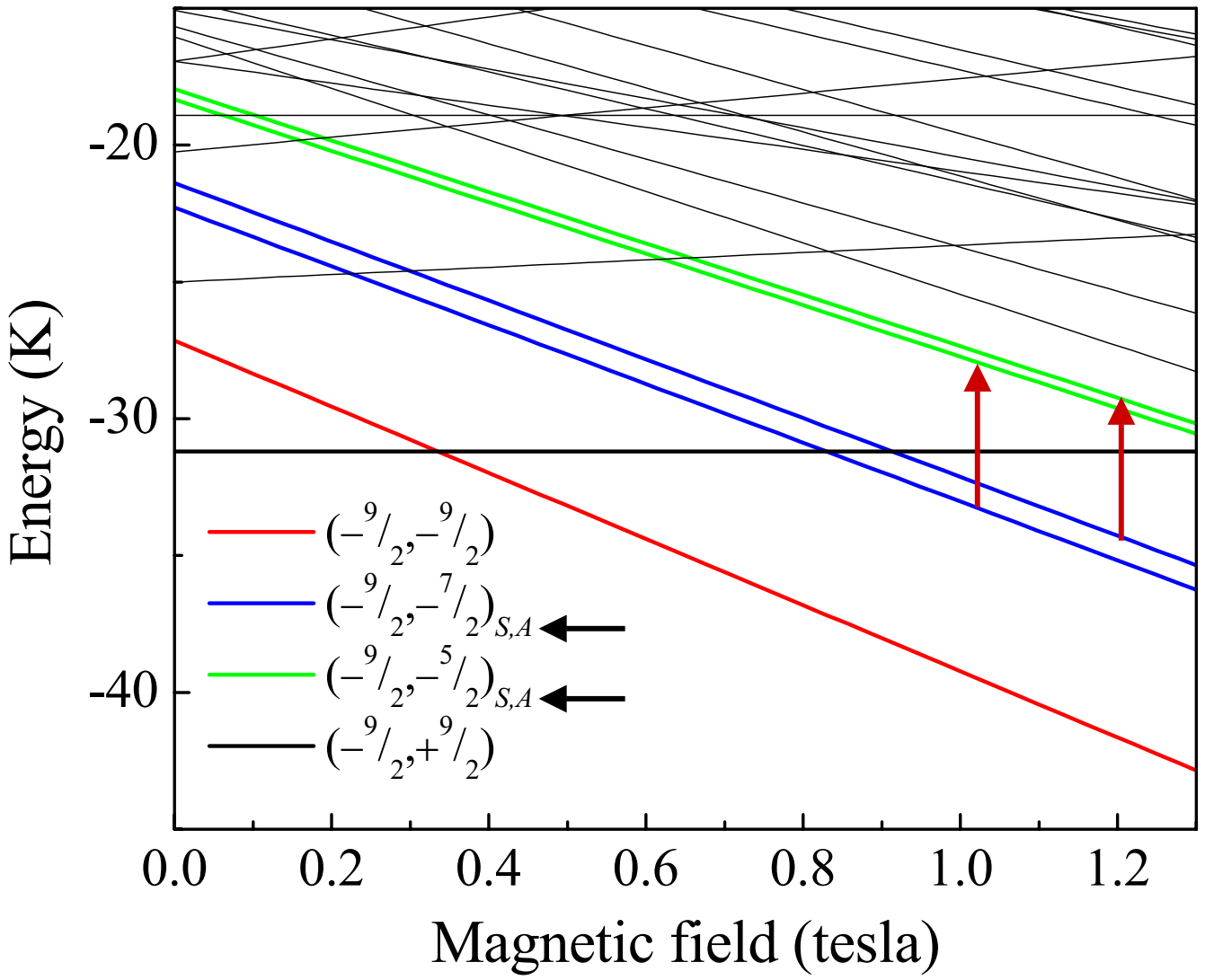

Look for additional splitting (multiplicity) and symmetry effects (selection rules) in EPR.

Clear evidence for coherent transitions involving both molecules

$$\hat{H}_D = \left[\hat{H}_{S1} + \hat{H}_{S2} + J\hat{S}_{z1}\hat{S}_{z2}\right] + \tfrac{1}{2}J\left(\hat{S}_1^+\hat{S}_2^- + \hat{S}_1^-\hat{S}_2^+\right)$$

$f = 145$ GHz

Experiment

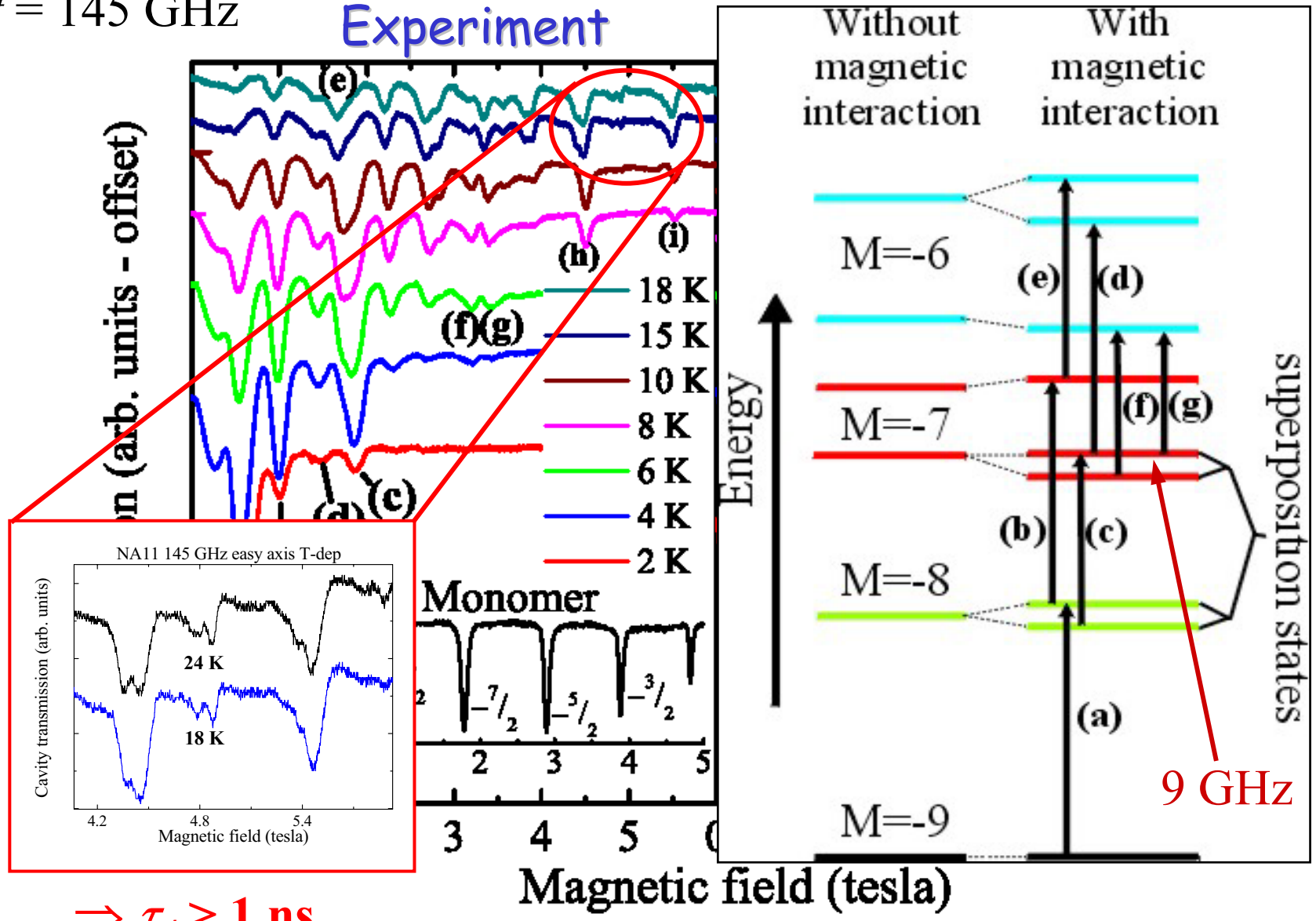

$\Rightarrow \tau_\phi > 1$ ns

S. Hill *et al.*, *Science* **302**, 1015 (2003)

Summary and conclusions

- Very powerful combination of experimental capabilities for studies of polynuclear transition-metal complexes:
  - tunable high-frequency millimeter and sub-millimeter-wave sources;
  - cavity perturbation and broad-band quasioptics;
  - high magnetic fields;
  - oriented single-crystal capabilities;
  - and variable temperatures.
- Improved understanding of various Mn_{12} complexes
- Thorough characterization of Ni_4 SMM
- Demonstration of entanglement between two Mn_4 SMMs

Useful references:

Mn_{12}-Ac review:	del Barco et al., arXiv/cond-mat/0404390 (JLTP, 2005)
More on Mn_{12}:	Petukhov et al., Phys. Rev. B **70**, 054426 (2004)
	Takahashi et al., Phys. Rev. B **70**, 094429 (2004)
	Hill et al., Phys. Rev. Lett. **90**, 217204 (2003)
Ni_4 systems:	Yang et al., Inorg. Chem., May 2005 (cond-mat/0502564)
Mn_4 Dimer:	Hill et al., Science **302**, 1015 (2003)

Many collaborators

...illustrates the interdisciplinary nature of this work

UF Physics

Rachel Edwards
Alexey Kovalev
John Lee

Susumu Takahashi
Jon Lawrence
Norman Anderson
Tony Wilson
Cem Kirman

Shaela Jones
Sara Maccagnano

FSU Chemistry

Naresh Dalal

Micah North
David Zipse
Randy Achey
Chris Ramsey

NYU Physics

Andy Kent

Enrique del Barco

UF Chemistry

George Christou

Nuria Aliaga-Alcalde
Monica Soler
Nicole Chakov
Sumit Bhaduri
Muralee Murugesu
Alina Vinslava
Dolos Foguet-Albiol

UCSD Chemistry

David Hendrickson

En-Che Yang
Evan Rumberger

Also: Kyungwha Park (NRL)
Wolfgang Wernsdorfer (Grenoble)
Mark Novotny (MS State U)
Per Arne Rikvold (CSIT - FSU)

Sixth International Symposium on Crystalline Organic Metals, Superconductors, and Ferromagnets

Key West, Florida
September 11-16, 2005
Wyndham Casa Marina Resort

Hosted by the J.E. Crow National High Magnetic Field Laboratory

Overview

ISCOM is the preeminent forum for interdisciplinary discussions of the Chemistry, Physics, Materials Science and Technology of crystalline molecular solids:

- **Synthesis of New Molecules**
- **Molecular Materials and Crystal Engineering**
- **Molecular Magnetism**
- **Physics of Low Dimensional Metals and Superconductors**
- **Magnetic Field-Induced Phenomena**
- **Thin Films and Devices**

Chairman and Secretary
James Brooks (FSU/NHMFL)

Co-chairs:
Luis Balicas (NHMFL)
Naresh Dalal (FSU)
Steven Hill (Univ. Florida/NHMFL)
Michael Naughton (Boston College)
Stuart Brown (U.C. Los Angeles)
Neil Harrison (LANL/NHMFL)
Janice Musfeldt (UT, Knoxville)

4th International Conference on Low Temperature Physics

10 - 17 August 2005 Orlando, Florida, USA
hosted by Department of Physics, University of Florida, Gainesville

Conference Chair: Gary G. Ihas Conference Secretary: Mark W. Meisel